Developmental Biology 448 (2019) 119–135

Contents lists available at ScienceDirect

Developmental Biology

journal homepage: www.elsevier.com/locate/developmentalbiology

Original research article

Positioning a multifunctional basic helix-loop-helix transcription factor within the *Ciona* notochord gene regulatory network

Jamie E. Kugler[1,2], Yushi Wu[1], Lavanya Katikala, Yale J. Passamaneck[3], Jermyn Addy, Natalia Caballero, Izumi Oda-Ishii[4], Julie E. Maguire, Raymond Li, Anna Di Gregorio[*]

Department of Basic Science and Craniofacial Biology, New York University College of Dentistry, 345 E 24th Street, New York, NY 10010, USA

ARTICLE INFO

Keywords:
bHLH
Brachyury
Ciona
Enhancer
Gene regulatory network
Notochord

ABSTRACT

In a multitude of organisms, transcription factors of the basic helix-loop-helix (bHLH) family control the expression of genes required for organ development and tissue differentiation. The functions of different bHLH transcription factors in the specification of nervous system and paraxial mesoderm have been widely investigated in various model systems. Conversely, the knowledge of the role of these regulators in the development of the axial mesoderm, the embryonic territory that gives rise to the notochord, and the identities of their target genes, remain still fragmentary. Here we investigated the transcriptional regulation and target genes of Bhlh-tun1, a bHLH transcription factor expressed in the developing *Ciona* notochord as well as in additional embryonic territories that contribute to the formation of both larval and adult structures. We describe its possible role in notochord formation, its relationship with the key notochord transcription factor Brachyury, and suggest molecular mechanisms through which Bhlh-tun1 controls the spatial and temporal expression of its effectors.

1. Introduction

Basic helix-loop-helix (bHLH) transcription factors play relevant roles in a variety of developmental and evolutionarily conserved processes, including cell-fate specification and tissue differentiation (Gyoja, 2017). bHLH proteins contain basic amino acids that facilitate binding to DNA and a helix-loop-helix domain that mediates their homo- or heterodimerization; this process can, in turn, modify their effect on the transcription of their target genes (Wang and Baker, 2015). The dimerization of bHLH proteins brings the DNA-binding domains together, allowing them to bind a specific core nucleotide sequence, the E-box (CANNTG), and thus trigger either transcriptional activation or repression (e.g., Jones, 2004; Suzuki et al., 2014). Expression studies suggest that the notochord of the tunicate *Ciona*, an invertebrate chordate particularly amenable for studies of embryogenesis, development and evolution (Passamaneck and Di Gregorio, 2005; Jiang and Smith, 2007; Lemaire et al., 2008), expresses approximately less than one hundred distinguishable transcription factor genes (e.g., Satou et al., 2001; Kusakabe et al., 2002; Imai et al., 2004; Kugler et al., 2008; José-Edwards et al., 2011; Reeves et al., 2017). Among these is *Bhlh-tun1* (formerly *Orphan bHLH-1*), which is expressed robustly in the *Ciona* notochord beginning around late gastrulation (Satou et al., 2001; Imai et al., 2004). The predicted Bhlh-tun1 protein does not evidently meet the criteria for any of the current monophyletic bHLH groupings, which are based on conserved features such as the presence of a leucine zipper (Jones, 2004); instead, Bhlh-tun1 is composed of only 139 amino acids, half of which are part of the basic DNA-binding domain. The appearance of *Bhlh-tun1* transcripts in the notochord precursors closely follows the onset of notochord expression of the *Ciona* counterpart of *Brachyury* (*Ci-Bra*), a gene that plays an evolutionarily conserved, major role in notochord formation in all chordates analyzed thus far (Kispert et al., 1995; Corbo et al., 1997;

Abbreviations: bp, base pair(s); bHLH, basic helix-loop-helix; CNS, central nervous system; cpm, counts per minute; CRM, *cis*-regulatory module; Ctrl, control; ECM, extracellular matrix; EST, expressed sequence tag; GFP, green fluorescent protein; GRN, gene regulatory network; GST, glutathione S-transferase; kb, kilobase(s), or 1000 base pairs; hpf, hours post-fertilization; h., hour(s); ORF, open reading frame; PCR, polymerase chain reaction; RACE, rapid amplification of cDNA ends; TXF, transcription factor; WMISH, whole-mount *in situ* hybridization; X-Gal, 5-bromo-4-chloro-3-indolyl-beta-D-galactopyranoside

* Corresponding author.
E-mail address: adg13@nyu.edu (A. Di Gregorio).
[1] Equal contribution.
[2] Present address: NIH/NIDCR, 30 Convent Drive, rm. 5A505, Bethesda, MD 20894, USA.
[3] Present address: US Bureau of Reclamation, Reclamation Detection Laboratory for Exotic Species, Denver, CO 80225, USA.
[4] Present address: Department of Zoology, Graduate School of Science, Kyoto University, Kyoto 606-8502, Japan.

https://doi.org/10.1016/j.ydbio.2019.01.002
Received 1 August 2018; Received in revised form 27 December 2018; Accepted 1 January 2019
Available online 18 January 2019
0012-1606/

Satoh et al., 2012;Nibu et al., 2013). In addition to being expressed in the notochord, Bhlh-tun1 is expressed in the anterior-most region of the sensory vesicle, which is part of the pre-metamorphic CNS and contains the anlagen of the oral siphon, a structure that develops after metamorphosis, as well as in the developing epidermis. Expression in the epidermal midline begins at neurula and persists throughout the late tailbud and larval stages (Imai et al., 2004; Roure and Darras, 2016). It is noteworthy that, differently from Ci-Bra, Bhlh-tun1 is robustly expressed also after metamorphosis, well after the disappearance of the notochord. Expression of Bhlh-tun1 has been reported in the inner atrial siphon muscle precursors (iASMP) of late swimming larvae (around stage 29; Hotta et al., 2007), and is later detected in the oral siphon muscles and their precursors (Razy-Krajka et al., 2014; Tolkin and Christiaen, 2016).

The early onset of notochord expression of Bhlh-tun1 and the occupancy of its genomic locus by Ci-Bra, which was revealed by ChIP-chip experiments (Kubo et al., 2010), led us to hypothesize that Bhlh-tun1 might act as a transcriptional intermediary of Ci-Bra and thus be part of the Ci-Bra-downstream notochord gene regulatory network (GRN). To test this hypothesis, we sought to isolate and characterize notochord enhancer(s) within the *Bhlh-tun1* genomic locus, and to identify genes that might be controlled by Ci-Bra through Bhlh-tun1. We analyzed the phenotype caused by the overexpression of Bhlh-tun1 in the notochord and, through microarray screens, we identified potential target genes of Bhlh-tun1. As expected, these genes are expressed not only in the notochord, but also in epidermis and developing CNS, and in juvenile organs after metamorphosis.

The results of this study position Bhlh-tun1 within the Ci-Bra-downstream regulatory hierarchy responsible for notochord development, and shed light on the role of this transcription factor in modulating the expression of genes involved in the morphogenesis of this structure.

2. Materials and methods

2.1. Animals and electroporations

Adult *Ciona robusta* (formerly *Ciona intestinalis* species A) were purchased from Marine Research and Educational Products (M-REP; Carlsbad, CA) and kept at 16 °C in recirculating artificial seawater. Culturing, electroporations, fixation and staining were carried out as previously described (Oda-Ishii and Di Gregorio, 2007). To obtain transgenic juveniles, electroporated embryos were transferred to non-coated Petri dishes after hatching and reared in filtered artificial seawater for 9 days (approximately early juvenile I stage; Hotta et al., 2007), in the presence of diluted food particles and a mixture of penicillin/streptomycin. The seawater was replaced every 2–3 days to avoid contamination. Each construct was tested a minimum of 4 times on different batches of embryos, in parallel with the empty pFBΔSP6 vector as a control (Oda-Ishii and Di Gregorio, 2007). A minimum of 50 fully developed, X-Gal stained embryos were scored per experiment, for each construct.

2.2. Plasmids construction

The *Bhlh-tun1* 1.7-kb 5′-flanking region was PCR-amplified from *Ciona robusta* genomic DNA using the following primers (restriction sites are underlined):

bHLH1-1.7kb-5: 5′-tccactcgagCTGCCACGTTACTTCTCCATTC-3′
bHLH1-1.7kb-3: 5′-cctgtctagaCAATAGTCAACGCGTATGTTAC-3′

then digested and ligated as an XhoI/XbaI fragment into the pFBΔSP6 vector (Oda-Ishii and Di Gregorio, 2007). Subsequent deletions were made by restriction enzyme digestion or by PCR amplification. Mutant versions of the minimal enhancer regions were generated by PCR amplification. Additional oligonucleotide sequences are available upon request.

To generate the *Bra > Bhlh-tun1* construct, the *eGFP* coding sequence was excised from the 3.5-kb *Ci-Bra > eGFP* plasmid (Corbo et al., 1997) by digestion with *Not*I and *Blp*I, and the remaining plasmid was ligated with the annealed oligos:

Not.Apa.Spe.linker.F:

5′-GGCCGCGGAGGAGGGCCCGGAGGAACTAGTGGAGGAGC-3′
Not.Apa.Spe.linker.R
5′-TCAGCTCCTCCACTAGTTCCTCCGGGCCCTCCTCCG-3′

to generate the vector p3.5Bra.link.

The coding region of *GFPci* (*Ciona* codon-optimized GFP), which is considerably brighter than *eGFP* (Zeller et al., 2006), was amplified as previously described (Passamaneck et al., 2009) and cloned into the SpeI/BlpI sites of p3.5Bra.link to generate the p3.5Bra.GFP intermediate vector. The *Bhlh-tun1* coding sequence was PCR-amplified with the primers:

bHLH1.F.Apa: 5′-tggtagggcccATGGTTAAAGCGAGCCCGATCAAAGA-3′
and
bHLH1.R.Spe: 5′-ggttactagtCTCTCGCGTTCTGGAATTGGAAT-3′

digested with *Apa*I/*Spe*I and ligated with the p3.5Bra.GFP intermediate vector to create the *Bra > Bhlh-tun1::GFPci*.

To construct the *FoxA.a > Bhlh-tun1::Venus* plasmid, the Venus coding region (Nagai et al., 2002) was amplified with the primers:

Venus.F.Spe5′-aaggactagtATGGTGAGCAAGGGCGAGGAG-3′ and
Venus.R.Blp5′-cgaccggcgctcagcTTACTTGTACAGCTCGTCCATGCC-3′

The resulting fragments were digested with *Not*I/*Blp*I respectively, then cloned into the NotI/BlpI sites of p2.5FoxA.a.link to produce the final *FoxA.a > Bhlh-tun1::Venus* construct.

To identify a notochord CRM linked to *Claudin16/17/19* (KH.C5.124), a genomic DNA fragment spanning 300 bp located in the 5′-flanking region of this gene was PCR-amplified from *C. robusta* DNA using the following primers:

Claudin Forward: 5′-acgtctcgagCCACTTACATTCATCAAACAACAA-3′
Claudin Reverse: 5′-acgttctagaCATATATGGCGTGACCAAGTT-3′

The resulting PCR product was digested and ligated into the *Xho*I/*Xba*I sites of the pFBΔSP6 vector (Oda-Ishii and Di Gregorio, 2007).

2.3. RNA probes synthesis

Antisense RNA probes were synthesized using as templates cDNAs from the available *Ciona* EST collections (Satou et al., 2001; Gilchrist et al., 2015). cDNAs not represented in EST collections were amplified by RT-PCR from *Ciona* RNAs, essentially as previously described (Oda-Ishii and Di Gregorio, 2007); primer sequences are available upon request. For antisense RNA probe synthesis, one microgram of each purified plasmid DNA was used as a template for *in vitro* transcription in the presence of T7 RNA polymerase and 11-digoxigenin-UTP (Roche Applied Science, Indianapolis, IN, USA), according to the manufacturer's instructions.

2.4. Whole mount in situ hybridization (WMISH)

WMISH experiments were performed as previously described (Oda-Ishii and Di Gregorio, 2007), using a hybridization temperature

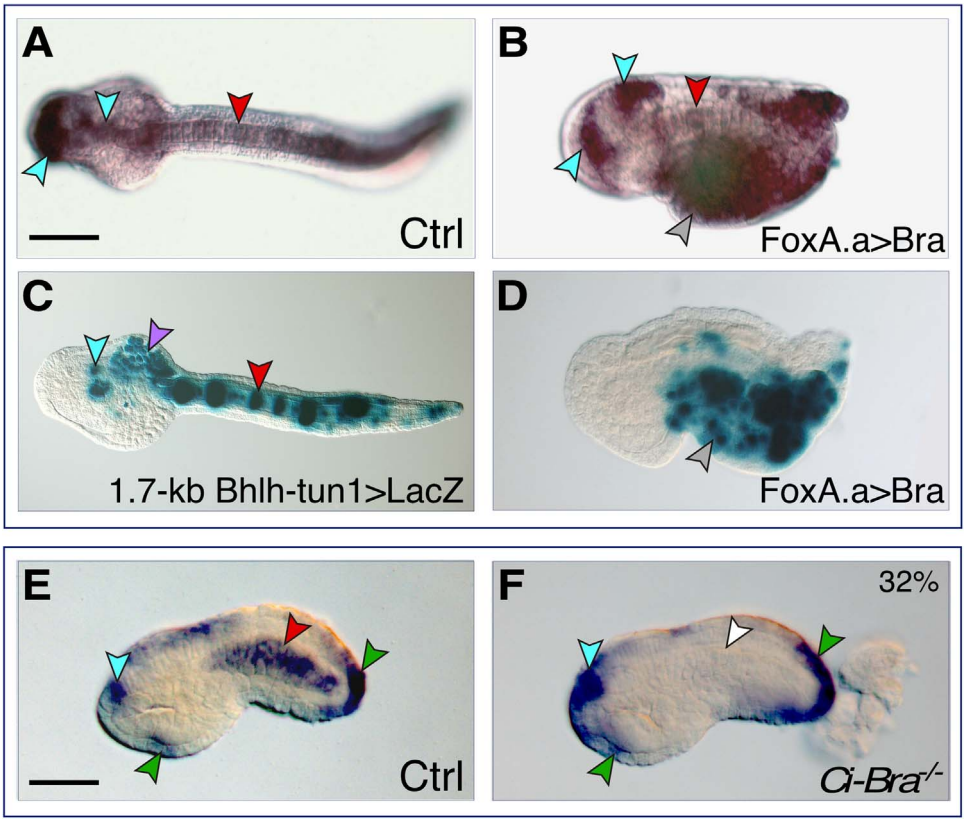

Fig. 1. The Ci-Bra-dependent expression of Bhlh-tun1 is recapitulated by its *cis*-regulatory region. (A,B) Whole-mount *in situ* hybridizations (WMISH) of late tailbud II embryos (stages according to Hotta et al., 2007) with a *Bhlh-tun1* digoxygenin-labeled antisense RNA probe. (A) Control embryo. (B) Transgenic embryo carrying the *Ci-FoxA.a > Ci-Bra* construct (abbreviated as *FoxA.a > Bra*). (C,D) Whole-mount late tailbud II embryos stained to detect beta-galactosidase activity after having been electroporated with a 1.7-kb genomic fragment from the 5′-upstream region of *Bhlh-tun1*, either alone (C), or in combination with the *FoxA.a > Bra* construct (D). (E,F) WMISH of early tailbud I embryos with the same probe used in (A,B). (E) Control embryo. (F) Mutant embryo, presumably with *Ci-Bra*$^{-/-}$ genotype, displaying a shorter tail and malformed notochord compared to stage-matched controls. These embryos lack expression of *Bhlh*-tun1 in the notochord (white arrowhead), yet they retain expression of this gene in its additional expression domains (arrowheads). Arrowheads are color-coded as follows: red, notochord; blue, CNS; green, epidermis; purple, mesenchyme; grey, cells that are misplaced to the ventral region of the embryo as a consequence of the ectopic expression of Ci-Bra in CNS and endoderm precursors and its over-expression in notochord cells. White, notochord cells showing no expression of *Bhlh-tun1*. All embryos are oriented with anterior to the left and dorsal up. Scale bars indicate approximately 100 μm in A and 50 μm in E. Ctrl, control wild-type embryo.

of 42 °C. After the detection reactions were satisfactorily completed (~4–48 h.), embryos were washed 6 times in 100% ethanol, rinsed briefly in xylenes, and mounted in Permount (Sigma, St. Louis, MO, USA).

2.5. Microarray screens

For the microarray screens, approximately 200 embryos expressing either the *FoxA.a > Bhlh-tun1::Venus* or the *Bra > Bhlh-tun1::GFPci* transgenes were manually selected under an epifluorescent microscope and RNA was extracted using the RNeasy kit (Qiagen, Valencia, CA), following the manufacturer's protocol. Control RNA was extracted from stage-matched non-electroporated embryos from the same clutch, cultured in parallel. One microgram of total RNA per sample was labeled with either Cy3 or Cy5 and hybridized to 6 slides of a *Ciona robusta* microarray (Agilent Technologies, Santa Clara, CA), essentially as previously described (Azumi et al., 2003; Yamada et al., 2005). The results were analyzed using the GeneSpring software (Agilent Technologies).

2.6. Reverse transcription quantitative PCR (qRT-PCR)

For qRT-PCR, we extracted RNA from stage 19/early tailbud stage I (Hotta et al., 2007) wild-type embryos and embryos from the same clutch electroporated with the *FoxA.a > Bhlh-tun1* plasmid and reared in parallel (9.3 h. cultures at 18 °C). In a second set of experiments, RNA was extracted from wild-type and transgenic embryos at stage 23/late tailbud I (12 h. cultures at 18 °C) (Hotta et al., 2007). RNAs were transcribed to cDNA using the Cell-to-Ct kit (Thermo Fisher Scientific, USA). The cDNA samples obtained were then analyzed by quantitative PCR using the SYBR green method (Thermo Fisher Scientific, USA). Details of the experimental results are listed in Table S1, oligonucleotide sequences can be found in Table S2.

2.7. Protein purification

The nucleotide sequence encoding the entire Bhlh-tun1 protein was amplified from *Ciona* cDNA using primers (restriction sites are underlined):

bHLH1-CDS-5: 5′-gccagaattcGCAAAAATGGTTAAAGCGAGCCCGATC-3′
bHLH1-CDS-3: 5′-tccactcgagGATTCACTCTCGCGTTCTGGAATTG-3′

and cloned in-frame with a GST tag into the XhoI/EcoRI sites of the pGEX-4T-2 expression vector (GE Healthcare, Piscataway, NJ). The resulting plasmid was transformed into chemically competent BL21 (DE3) *E. coli*. Bacteria were grown at 25 °C, and protein expression was induced by adding 0.5 mM IPTG to the medium for 3 h. The GST-Bhlh-tun1 fusion protein was purified from crude bacterial extracts using Glutathione Sepharose 4B beads (GE Healthcare, Piscataway, NJ) according to the manufacturer's instructions, and eluted in 50 mM

Tris pH 8.0 containing 10 mM reduced glutathione.

2.8. Electrophoretic mobility shift assay (EMSA)

For the EMSA shown in Fig. S2, the following double-stranded oligonucleotides were used (only the 5′-3′ strand is reported):

5′- cagatcgtcCAATTGctacttctg -3′ (AT core E-box)
5′- ttaaaatatCACATGatatagagg -3′ (CA core E-box)
5′- cagttcaatCACTTGtattaatag -3′ (CT core E-box)
5′- atctctaagCATATGttctttaat -3′ (TA core E-box)
5′- aaattggccCATGTGgtttaaaac -3′ (TG core E-box, different flanking)
5′- tggtataaaCATTTGaaagaatat -3′ (TT core E-box)

Other CANNTG sequences were used in separate experiments with similar results; cold competition assays confirmed binding specificity (data not shown). Complementary oligonucleotides were annealed, radioactively labeled and purified as previously described (Dunn and Di Gregorio, 2009). Protein-DNA complexes were formed on ice for 30 min, in the presence of ~3×10^4 cpm of each probe and 80 ng of the GST-Bhlh-tun1 fusion protein. The complexes were fractionated on 5% polyacrylamide/0.5× TBE gels and visualized by autoradiography.

3. Results

3.1. Expression of Bhlh-tun1 in notochord cells is dependent upon Ciona Brachyury

We hypothesized that the notochord expression of Bhlh-tun1 (KH.C7.269; Dehal et al., 2002; Satou et al., 2008) might be dependent upon Ci-Bra, based on the observation that the strong expression of Bhlh-tun1 in the notochord begins around the late gastrula stage, 2–3 cell divisions after the onset of Ci-Bra transcription, and continues until the late tailbud stages (Fig. 1A). To test this hypothesis, the *Bhlh-tun1* expression pattern was analyzed in embryos electroporated with the *FoxA.a > Bra* misexpression construct. This construct has been shown to activate ectopic transcription of *Ci-Bra* in the CNS and endoderm (Takahashi et al., 1999), thus giving the embryos a characteristic phenotype (Fig. 1B,D), and has been employed for a subtractive screen that led to the identification of 45 notochord genes that respond to Ci-Bra (Hotta et al., 2000, 2008). Embryos electroporated with *FoxA.a > Bra* and hybridized *in situ* with the *Bhlh-tun1* probe showed ectopic expression of this gene, indicating that *Bhlh-tun1* responds to the misexpression of Ci-Bra (Fig. 1B). These results prompted the search for a Ci-Bra-downstream notochord *cis*-regulatory module (CRM) within the *Bhlh-tun1* locus. To this aim, a 1.7-kb DNA fragment located 5′ of the *Bhlh-tun1* coding region was cloned upstream of the *Ci-FoxA.a* basal promoter fused to the *LacZ* reporter gene (Oda-Ishii and Di Gregorio, 2007) and tested *in vivo* by electroporation in *Ciona* zygotes. In transgenic embryos, this genomic region recapitulates the strong expression of *Bhlh-tun1* in notochord cells and sensory vesicle, and displays expression in mesenchyme, which is likely ectopic and attributable to the vector (Fig. 1C; see also Fig. 2C). When this 1.7-kb CRM was co-electroporated into 1-cell stage embryos along with the *FoxA.a > Bra* construct, ectopic reporter gene expression was detected (Fig. 1D), suggesting that this CRM was responsive to Ci-Bra, similarly to *Bhlh-tun1*. To confirm these results, we assessed the effects of *Ci-Bra* depletion on the notochord expression of *Bhlh-tun1*, by performing WMISH in parallel on wild-type controls and on mutant embryos carrying a null allele of *Ci-Bra*, generated in *Ciona robusta via* ENU mutagenesis (Chiba et al., 2009) (kindly provided by Dr. William Smith; University of California, Santa Barbara) using a *Bhlh-tun1* antisense RNA probe synthesized using as a template EST clone 69O09. In total, 456 embryos, which included heterozygous and homozygous mutants, were scored for notochord staining. Of these, 308 (~68%) showed notochord expression of *Bhlh-tun1* and 148 (~32.5%) displayed a shorter tail compared to stage-matched controls and lacked expression of *Bhlh-tun1* in their notochord (Fig. 1E,F). Before metamorphosis, *Bhlh-tun1* is also strongly expressed in the epidermal midline (Imai et al., 2004; Roure and Darras, 2016) and in parts of the sensory vesicle, the anterior-most region of the CNS (Imai et al., 2004). Expression of *Bhlh-tun1* in these structures remained unaltered in Ci-Bra mutant embryos, thus providing an internal control for the WMISH experiments (Fig. 1F). Remarkably, in addition to direct reporter gene expression in notochord, sensory vesicle and mesenchyme, the 1.7-kb genomic region is also active in both siphon primordia in hatched larvae (Fig. S1A,B). In juveniles, this region directs staining in cells of the developing oral siphon (Fig. S1C,C′) and in part of the atrial siphon muscle (Fig. S1D,D′).

3.2. Enhancer analysis reveals the minimal sequences required for Bhlh-tun1 expression in the notochord

We tested different genomic regions from the *Bhlh-tun1* locus for *cis*-regulatory activity (Fig. 2), in addition to the 1.7-kb region shown in Fig. 1. We found that neither the small coding region of *Bhlh-tun1* (1.2-kb fragment, Fig. 2) nor a 1-kb region downstream of it (1-kb fragment, Fig. 2) produced staining *in vivo*. However, a 995-bp fragment located 0.9 kb upstream of the 1.7-kb CRM directed *LacZ* expression in tail epidermis (Fig. 2A). Epidermal staining is not detected in embryos electroporated with the 1.7-kb CRM (Fig. 2B), and is absent in control embryos electroporated with the empty vector (Fig. 2C), which suggests that this separate epidermal CRM might act in combination with the former one to produce the composite expression pattern of *Bhlh-tun1*. Sequence inspection revealed that the 1.7-kb notochord CRM contained several generic TNNCAC candidate Ci-Bra binding sites (Di Gregorio and Levine, 1999; Katikala et al., 2013), as well as putative binding sites for another evolutionarily conserved notochord transcription factor, Ci-FoxA.a (Passamaneck et al., 2009; José-Edwards et al., 2015). In order to identify the most relevant ones among these putative binding sites, and to analyze their individual contributions and possible synergistic activities, a 144-bp sequence that still yielded reliable notochord staining in > 50% of the electroporated embryos was identified through serial truncations (Fig. 2 and data not shown). This 144-bp sequence contained three putative binding sites for Ci-Bra and 2 for Ci-FoxA.a, and therefore was subjected to mutation analysis (Fig. 2). A total of 16 constructs, containing individual and compound mutations of all the Ci-Bra and Ci-FoxA.a putative binding sites were prepared and tested *in vivo* (Fig. 2 and data not shown). This analysis showed that removal of all the Ci-Bra binding sites from the 144-bp *Bhlh-tun1* notochord CRM caused a reduction of notochord staining, but was not sufficient to abolish its activity, and neither was the combination of these mutations with the removal of the Ci-FoxA.a binding sites. Through further truncations we identified a 58-bp minimal enhancer region that still elicited notochord staining (Fig. 2D). Additional mutation analysis was carried out on this 58-bp region and indicated that an ATTA minimal sequence, which is the core binding site for transcription factors of the homeodomain family, was necessary for notochord activity (Fig. 2E,F). Removal of 9 bp encompassing the ATTA sequence from the 58-bp minimal region completely eliminated notochord staining, leaving only vector background staining (Fig. 2G, compare to Fig. 2D). When tested in isolation as part of a 24-bp fragment that lacked all Ci-Bra and Ci-FoxA.a sites, the 9-bp sequence necessary for activity was not sufficient to trigger notochord expression (data not shown), suggesting that this homeodomain binding site is not working independently, but rather in combination with the Ci-Bra and Ci-FoxA.a binding sites found in the 58-bp sequence.

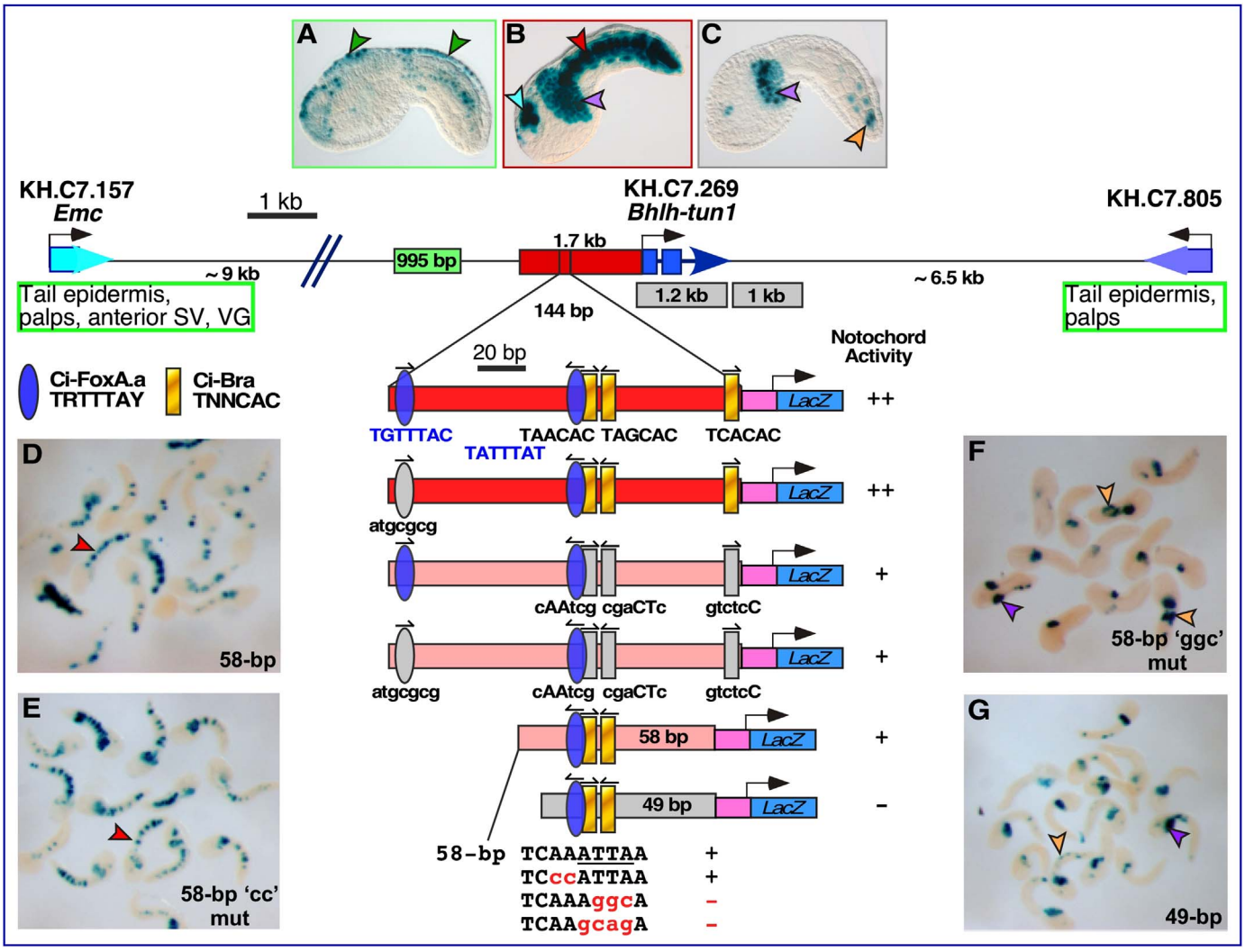

Fig. 2. Identification and characterization of an epidermis CRM and a notochord CRM from the *Bhlh-tun1* genomic locus. Schematic representation of the *Bhlh-tun1* locus and its genomic surroundings, which include the flanking genes KH.C7.157 (*Emc*; light blue; Imai et al., 2004) and KH.C7.805 (lilac; Brozovic et al., 2016). Exons are indicated as blue boxes, introns are shown as lines between them. Two enhancer regions are depicted as compact bars, colored in green (epidermis) and red (notochord), respectively. Oblique lines indicated intervening genomic regions devoid of gene models that have not been depicted. Black bent arrows indicate the approximate transcription start sites. Within the red bar that represents the 1.7-kb CRM identified directly upstream of the *Bhlh-tun1* coding region, the 144-bp notochord CRM is indicated, and is then magnified and annotated with putative binding sites for Ci-FoxA.a (blue ovals, consensus sequence shown on the left side of the figure) and for Ci-Bra (yellow vertical bars). The specific sequences of these sites are indicated below the 144-bp CRM depiction (blue letters for Ci-FoxA.a binding sites, black for Ci-Bra), and mutant base pairs are indicated by lower-case letters. All fragments were cloned upstream of the *Ci-FoxA.a* basal promoter (pink box) driving the *LacZ* reporter gene (blue bar, annotated). Plus or minus signs in the 'Notochord Activity' column indicate the presence or absence of notochord staining related to each construct. Two plus signs indicate a qualitatively stronger notochord staining in > 50% of the electroporated embryos. (A-C) Mid-tailbud embryos electroporated at the 1-cell stage with either the 995-bp genomic fragment (green box) (A), or the *Bhlh-tun1* 1.7-kb CRM (red box) (B) or the empty pFBΔSP6 vector (C), fixed and stained with X-Gal. The image in Panel A is a composite of 3 microphotographs of the same embryo, photographed in different planes of focus, *z*-stacked using the ImageJ software (www.imagej.net). (D-G) Low-magnification microphotographs of representative transgenic embryos selected from larger batches to display the staining produced by the 58-bp minimal notochord enhancer fragment (D) and two of its mutant forms (E,F), alongside the 49-bp truncation that lacks notochord activity (G). Arrowheads are color-coded as in Fig. 1; orange arrowheads indicate muscle staining. SV, sensory vesicle; VG, visceral ganglion.

3.3. Insights into the function of Bhlh-tun1 in notochord formation

As a first step towards elucidating the function of *Bhlh-tun1* in notochord formation, we investigated whether Bhlh-tun1 possessed the ability to bind DNA specifically and autonomously. As mentioned above, Bhlh-tun1 is comprised primarily of a single helix-loop-helix DNA-binding domain, with minimal sequence on either side, according to the available *Ciona robusta* gene models (Dehal et al., 2002; Satou et al., 2008). We attempted both 5′- and 3′-RACE experiments (Frohman, 1993) to determine whether the gene model was correct, however no significant ORF was found beyond the predicted start and stop codons (data not shown). Next, in order to determine whether Bhlh-tun1 was able to bind DNA *in vitro*, we expressed and purified a GST-Bhlh-tun1 fusion protein, which was employed for electrophoretic mobility shift assays (EMSA) in the presence of radiolabeled double-stranded oligonucleotides containing E-box sequences (CANNTG) with different core sequences. EMSA experiments were repeated using probes of different length containing E-boxes of variable sequences in parallel with unrelated sequences, as well as in the presence of increasing amounts of unlabeled competitor double-stranded oligonucleotides. These assays confirmed that GST-Bhlh-tun1 is able to bind DNA *in vitro* and to specifically recognize E-boxes (Fig. S2 and data not shown). Having demonstrated that, in principle, Bhlh-tun1 could act as a transcription factor, we proceeded with the creation of gain-of-function constructs that could induce the over-expression of this protein in the notochord, and its ectopic expression in CNS and endoderm.

A construct able to over-express Bhlh-tun1 specifically in notochord

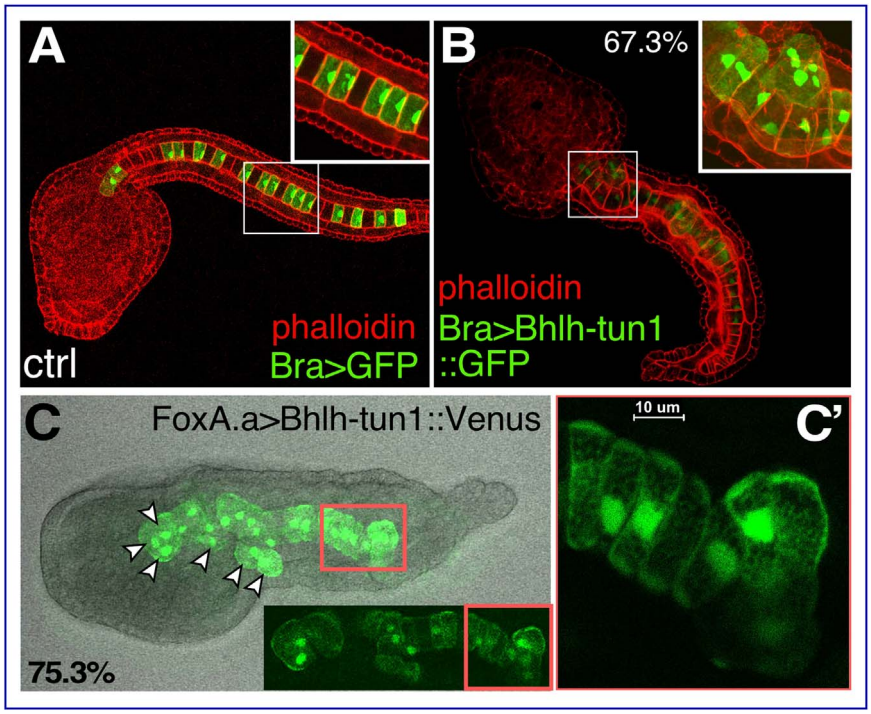

Fig. 3. Effects of the overexpression of Bhlh-tun1 on notochord and body plan formation. (A,B) Confocal microphotographs of *Ciona* embryos carrying the *Ci-Bra > GFP* neutral notochord marker, either alone (A) or in combination with the Ci-Bra > Bhlh-tun1::GFP construct (abbreviated as Bra > Bhlh-tun1::GFP) (B). Insets show close-ups of the regions boxed in white in each panel. The percentage of embryos displaying the notochord phenotype is reported in the top right corner of Panel B. Both embryos were stained with rhodamine-phalloidin as previously described (José-Edwards et al., 2013). (C) Overlap of bright-field and fluorescent confocal microphotographs of an embryo carrying the *FoxA.a > Bhlh-tun1* construct, representative of the phenotype induced by this transgene. All 40 notochord cells are fluorescent, and the panel shows a collapsed *z*-stack of their images acquired serially from the whole-mount embryo. The frequency of embryos displaying this phenotype is indicated in the bottom left corner. Inset shows the notochord cells in dark field (see also Supplemental Movie 1). The area boxed in red in (C) and in the inset is shown at higher magnification in (C′) to highlight the changes in cell shape induced by the overexpression of Bhlh-tun1. Scale bar in C′: 10 μm.

cells was created by cloning the *Bhlh-tun1* cDNA downstream of the 3.5-kb *Ci-Bra* promoter region (Corbo et al., 1997), and was electroporated in *Ciona* zygotes (Fig. 3A,B). In stage-matched control embryos (Fig. 3A), all 40 notochord cells are aligned into a single row as a result of the intercalation of two separate rows of 20 cells each (Fig. 3A, inset; Jiang and Smith, 2007). Most of the transgenic embryos over-expressing Bhlh-tun1 in notochord cells developed a kinked tail, whereby one or more regions of the notochord appeared to have undergone faulty intercalation (Fig. 3B, and inset therein). Time-course experiments revealed that these areas appeared at the early tailbud stage (Fig. S3A–D) and caused multiple kinks in the developing tail, which then resulted in visible bends in the tails of older tailbuds (Fig. S3E–H). A second construct aimed at ectopically expressing Bhlh-tun1 was obtained by cloning the fluorescent-tagged *Bhlh-tun1* downstream of the *Ci-FoxA.a* promoter region, which drives expression in notochord, endoderm, CNS and mesenchyme, and occasionally in a few muscle cells and small patches of epidermis (Di Gregorio et al., 2001 and data not shown) (Fig. 3C,C′). Approximately 75.3% of the embryos electroporated with the *FoxA.a > Bhlh-tun1* construct displayed the tail phenotype reported in Fig. 3C, whereby the notochord cells showed an irregular shape, had lost their colinearity and appeared spread out along the dorso-ventral axis, thus causing the tail to appear shorter and enlarged compared to control embryos (Fig. 3C,C′ and Supplemental Movie 1).

Supplementary material related to this article can be found online at doi:10.1016/j.ydbio.2019.01.002.

3.4. *Bhlh-tun1 influences transcription of genes expressed in embryonic tissues as well as in post-metamorphic structures*

We used a subtractive microarray screen to identify Bhlh-tun1 transcriptional targets that might be responsible for the notochord phenotype observed (Fig. 3). RNAs were extracted from embryos that in addition to over-expressing *Bhlh-tun1* in the notochord ectopically expressed this gene in CNS, endoderm and mesenchyme, through the construct *FoxA.a > Bhlh-tun1::Venus* (Fig. 3C,C′), and were used to hybridize a *Ciona robusta* custom microarray chip (Azumi et al., 2003; courtesy of Dr. Nori Satoh). RNAs extracted from stage-matched wild-type embryos were used as a control. The screen yielded 57 genes with expression fold-change higher than 2.0, and one of these genes was *Bhlh-tun1* itself. Expression data were available for 24 of the remaining 56 genes; we performed WMISH to determine the expression of the 32 uncharacterized genes, and discernible expression patterns were obtained for 27 of them; the remaining five genes yielded no detectable expression or unclear hybridization signals (Table 2). Fifteen of these newly identified expression patterns are shown in Fig. 4, which includes the expression of *Bhlh-tun1* at the mid-tailbud stage for reference (Fig. 4A). Fourteen of the 27 patterns identified in this study (~52%) included the notochord and/or its precursors, either specifically, or, more frequently, in combination with some regions of the epidermis and/or other tissues (Fig. 4B–M and data not shown); four genes were predominantly expressed in epidermis, and were not detected in the notochord (Fig. 4N–P and data not shown); two genes showed a diffuse, semi-ubiquitous pattern stronger in parts of the CNS (data not shown); seven genes were expressed in tissues not consistent with the pre-metamorphic expression pattern of *Bhlh-tun1*, such as endoderm and tail muscle (data not shown), but were not further analyzed in post-metamorphosis stages and might be expressed in post-metamorphic structures consistent with the *Bhlh-tun1* expression territories in juveniles. In addition, one possible cause for the detection of genes expressed in territories that are apparently devoid of *Bhlh-tun1* expression in wild-type embryos could be the leaky, sporadic ectopic activity of the *FoxA.a* promoter region, which is detected particularly in mesenchyme and tail muscle, and occasionally in

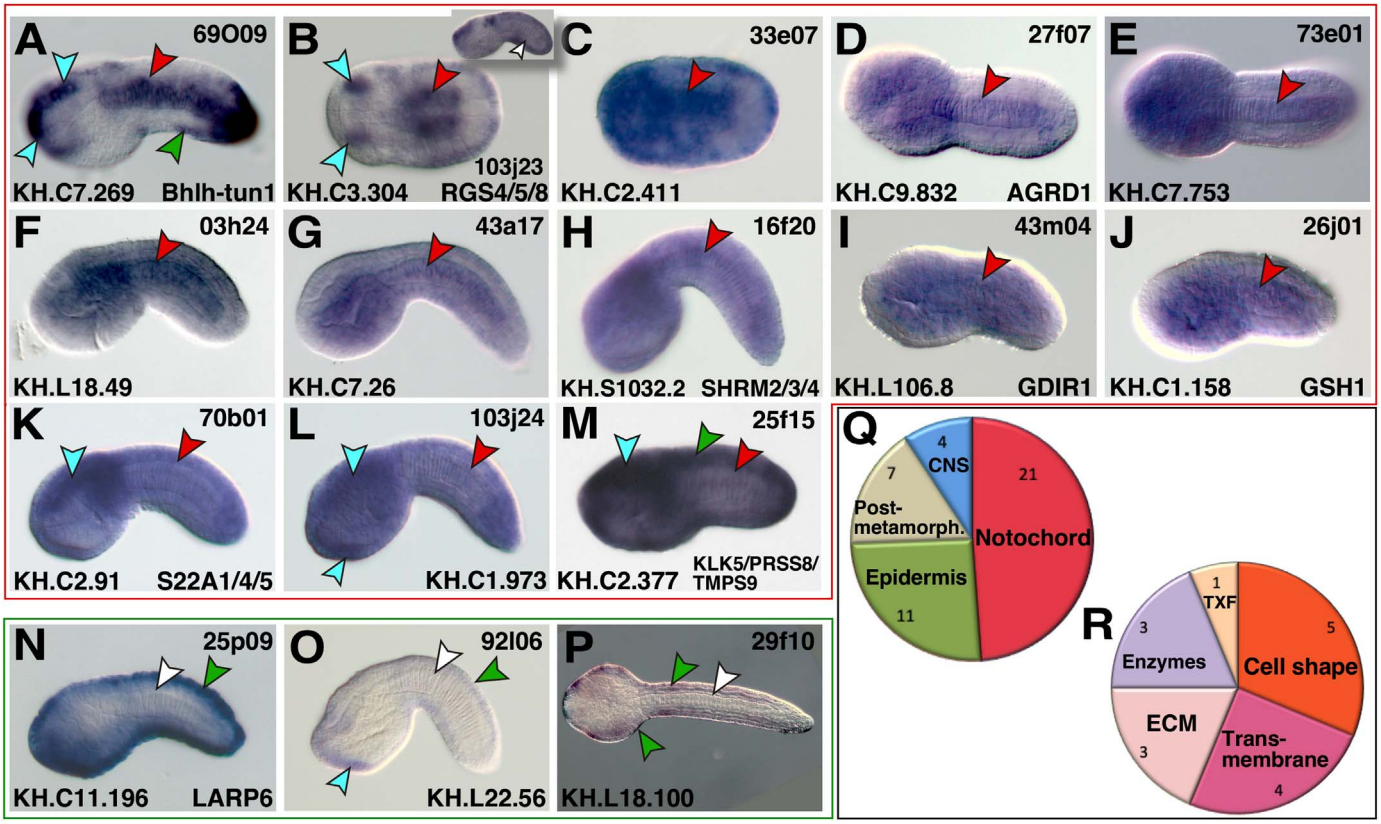

Fig. 4. Expression studies of putative Bhlh-tun1 target genes. (A-P) WMISH of *Ciona* embryos with digoxigenin-labeled antisense RNA probes for genes identified in the microarray screen. The EST clones used to generate each probe are reported in the top right corner of each panel. Most embryos are at tailbud stages (approximately ranging from mid-neurula to mid-tailbud II; Hotta et al., 2007); (B) dorsal view of mid-neurula embryo; (C) slightly lateral view of a mid-neurula embryo. Arrowheads are color-coded as in Fig. 1. (Q,R) Pie graphs showing the distribution within different expression territories of the genes identified as putative Bhlh-tun1 targets (Q) and the gene ontologies available for the 16 of the 21 Bhlh-tun1 targets expressed in notochord cells. Genes expressed in epidermis are framed in green (N-P). Current gene models are indicated in the bottom left corner of each panel; gene names, whenever available, are reported on the bottom right corner of each panel. TXF, transcription factor; ECM, extracellular matrix.

epidermis (Di Gregorio et al., 2001). We observed variability in the windows of expression of the presumptive Bhlh-tun1-downstream notochord genes, as some of them are expressed transiently, in particular during the early tailbud stages, while a few of these genes are expressed starting at late neurula and persist through the late tailbud stages. In the case of the larger group of genes that we tentatively classified as notochord genes, expression was detected predominantly in notochord but was also found in epidermis, and the relative expression levels in these tissues changed during different developmental stages. This was the case for KH.C3.304, which encodes RGS4/5/8, a GTPase activator; this gene is first detected in notochord and neural precursors, and by neurulation is expressed in notochord, neural folds, epidermis, and precursors of the anterior-most regions of the CNS and future palps (Fig. 4B and data not shown). At the mid-tailbud stage, expression fades from the notochord and persists in CNS and tail epidermis (inset in Fig. 4B). A similarly dynamic pattern was observed in the case of KH.C2.411, a seemingly ascidian-specific gene without clear homologies (Fig. 4C and data not shown).

The 27 published patterns (Table 1) included 7 notochord genes, 7 genes expressed in epidermis, one gene expressed in the sensory vesicle, 7 genes reportedly expressed after metamorphosis and 5 genes with diffuse/unclear expression. The post-metamorphic expression patterns encompass a variety of structures that are formed after metamorphosis, including branchial pharynx and atrial siphon muscle (Table 1, and references therein). Expression in the atrial siphon muscle is consistent with the expression of *Bhlh-tun1* in inner atrial siphon muscle precursors (Razy-Krajka et al., 2014; Tolkin and Christiaen, 2016). The combined results of previously published expression patterns consistent with the pre-metamorphic expression territories of *Bhlh-tun1* are summarized in Fig. 4Q together with the results of this study (Table 2).

In sum, the results of this study indicate that the expression of 21 notochord genes might be modulated by Bhlh-tun1 (Table 3). These genes include *MLKL* (mixed lineage kinase domain-like pseudokinase; KH.C4.411), which is first detected in early neurulae and remains notochord-specific throughout the late-tailbud stages (José-Edwards et al., 2013), and another highly expressed notochord gene, Beta-4-galactosyltransferase (Beta4GalT; Hotta et al., 2000; Katikala et al., 2013); on the other hand, *Lox1* displays diffuse, weak signal in notochord and additional expression in mesenchyme (KH.C8.476; Kugler et al., 2008), similarly to *AGRD1* (KH.C9.832; Fig. 4D), *GDIR1* (KH.L106.8; Fig. 4I), and *GSH1* (KH.C1.158; Fig. 4J).

Gene ontologies were available for 16 of the 21 Bhlh-tun1 target genes expressed in the notochord, and were individually analyzed in order to reconstruct the function of this factor in notochord development (Fig. 4R). Of note, one of these genes encodes for a transcription factor, Lhx3/4, which is a candidate activator of the *Bhlh-tun1* notochord CRM identified in this study (see above). In addition, GDIR1 is predicted to act as a Rho-GDP dissociation inhibitor, SWP70 for a regulator of cytoskeletal rearrangement, RGS4/5/8 and TBC3C/D are predicted GTPase activators, and SHRM2/3/4 encodes an actin-binding protein. These predicted regulators/effectors of cytoskeletal rearrangements have been tentatively grouped as 'regulators of cell-shape' in Fig. 4R. In addition, AGRD1 is a predicted transmembrane receptor, S22A1/4/5 is a transmembrane transporter, MLKL encodes for a predicted cation channel, and CLDN16/17/19 is a predicted claudin, a transmembrane component of intercellular tight junctions (grouped as 'transmembrane' in Fig. 4R). Lox1 is an

Table 1
Bhlh-tun1 putative target genes with published expression patterns.

KH gene model	Alternative/former Gene Name(s)	Latest Gene Name	Expression	Reference	Gene Ontology
KH.C1.90	SLC25A33/36	ODC; S2533; S2536	Weak staining in trunk endoderm; branchial pharynx of juveniles	Jose'-Edwards et al. (2013); Ogasawara et al. (2002).	Transmembrane transporter
KH.C4.411	MLKL	MLKL; RIPK1; TESK2	Notochord-specific	Jose'-Edwards et al. (2013)	Protein kinase, transmembrane cation channel
KH.C8.476	Ci-Lox1	LOXL2; LOXL3; LOXL4	Notochord	Kugler et al. (2008)	Scavenger receptor activity; protein-lysine 6-oxidase activity
KH.C14.163	Orphan bZip− 5	KH.C14.163	Mesenchyme, epidermis in larvae	Imai et al. (2004); Kusakabe et al. (2002)	N/A
KH.C2.208	USP6NL	TBC3C; TBC3D; US6NL	Notochord	Reeves et al. (2017)	GTPase activator activity
KH.L107.7	LHX1; LHX5; LMX1A (Ci-lhx1/5)	LHX1; LHX5; LMX1A	Sensory vesicle, visceral ganglion	Imai et al. (2004)	Transcription factor
KH.C6.198		AGRB2; HMCN1; TSP1	Trunk endoderm and epidermis	Satou et al. (2001)	Calcium ion binding
KH.C9.602		GCYA2; GCYB1; GCYB2	Ventral anterior sensory vesicle	Hudson and Lemaire (2001); Aniseed database, Brozovic et al. (2016)	Guanylate cyclase
KH.C1.653		CFA46	No data before metamorphosis; epidermis, pharyngeal gill, branchial pharynx of juveniles.	Ogasawara et al. (2002)	Cytoskeleton
KH.C14.201		ENTK; MALR1; MDGA1	Whole embryo, stronger in the trunk	Satou et al. (2001)	Integral to membrane
KH.C4.146		CTRB1; CTRB2; CTRL	Epidermis	Satou et al. (2001); Kusakabe et al. (2002)	Serine-type endopeptidase
KH.L96.11	TLE1; TLE3; TLE4 (Groucho; Groucho-2; Groucho-b)	TLE1; TLE3; TLE4	Whole embryo, no distinct zygotic signal; stomach and middle region of the pharynx in juveniles	Satou et al. (2001)	Negative regulation of transcription, DNA-dependent
KH.C14.414		PIM1; PIM2; PIM3	Epidermis	Satou et al. (2001)	ATP binding
KH.C1.1109		KH.C1.1109	Epidermis and oral siphon primordium, only tested in larvae	Kusakabe et al. (2002)	N/A
KH.L36.8		HMCN1; SEM5A; SEM5B	Epidermis, neural plate	Fujiwara et al. (2002); Kusakabe et al. (2002)	Calcium ion binding
KH.L9.13	MYF5/6 (Achaete-Scute a-like2)	KH.L9.13	Tail epidermis, epidermal sensory neurons, palps	Imai et al. (2004); Roure and Darras (2016)	Transcription factor
KH.S765.1	KH.S765.1 (Orphan bZip-3)	KH.S765.1	Maternal signal was observed ubiquitously mainly in the endodermal lineage; weak mesenchyme.	Imai et al. (2004)	Transcription factor
KH.C9.48	Ci-ZF004 aka CTGF; CYR61; NOV; WISP1	CTGF; CYR61; NOV; WISP1	Epidermis	Miwata et al. (2006)	Regulation of cell growth
KH.C4.326		SWP70	Notochord, epidermis, mesenchyme, nervous system	Satou et al. (2001)	Guanine nucleotide exchange factor, regulator of cytoskeletal rearrangement
KH.L34.9	HES1; HES2; HES4 (Ci-Hes; E(spl)/ hairy-c; Hes-like transcription factor)	HES1; HES2; HES4	Whole embryo, stronger in epidermis; likely maternal	Imai et al. (2004)	Transcription factor
KH.S1404.2		IRF4; IRF8; IRF9	Faint maternal whole embryo, later mesenchyme; branchial pharynx, hemocytes and endostyle of juveniles	Imai et al. (2004)	Transcription factor
KH.C11.44	Beta-4-galT	B4GT1; B4GT2; B4GT3	Notochord	Hotta et al. (2000)	Golgi membrane
KH.S215.4	LHX3/4	LHX3; LHX4; LHX5	Notochord, endoderm, a few muscle precursors, neural folds, anterior sensory vesicle, visceral ganglion	Imai et al. (2004); Kobayashi et al. (2010)	Transcription factor
KH.S655.4	Ci-META6-like	KH.S655.4	Notochord; endostyle of juveniles	Jose'-Edwards et al. (2013); Ogasawara et al. (2002).	N/A

Table 2
Results of WMISH experiments for Bhlh-tun1 putative target genes.

KH gene model	Alternative/former Gene Name(s)	Latest Gene Name	Expression	Classified as:	Reference	Figure	Gene Ontology
KH.L18.100	CSH1	KH.L18.100	Epidermis	Epidermis	This Study, EST 29f10	Fig. 4P	N/A
KH.S1032.2	SHROOM/3	SHRM2; SHRM3; SHRM4	Ubiquitous, slightly stronger in notochord and mesenchyme	Notochord	This Study, EST 16f20	Fig. 4H	Actin binding
KH.C11.711		KH.C11.711	Faint mesenchyme	Not consistent	This Study, EST 25L13	Data not shown	N/A
KH.C4.714		KH.C4.714	No expression	No expression	This Study, EST 44E08	Data not shown	N/A
KH.C3.469		HEBP2	Endoderm, possibly mesenchyme	Not consistent	This Study, EST 66O19	Data not shown	Mitochondrial membrane permeabilization
KH.C9.832	GPR133	AGRD1; AGRL2; LPHN3	Diffuse signal in the trunk, stronger in notochord	Notochord	This Study, EST 27F07	Fig. 4D	Transmembrane signaling receptor activity
KH.C2.377	MP1	KLK5; PRSS8; TMPS9	Diffuse staining, including epidermis and notochord	Notochord	This Study, EST 25f15	Fig. 4M	Serine-type endopeptidase
KH.C2.91	TPO1/2/3 (Ci-Organic cation/ carnitine transporter 2 like	S22A1; S22A4; S22A5	Ubiquitous, including notochord precursors, stronger in CNS	Notochord	This Study, EST 70b01	Fig. 4K	Transmembrane transporter
KH.C6.244	TNNC1 (Ci-TNC3)	CALM; TNNC1; TNNC2	Trunk mesenchyme, primary muscle	Not consistent	This Study, EST 69N23	Data not shown	Calcium ion binding
KH.C8.489	SI: DKEY-29D8.3	KH.C8.489	No expression	No expression	This Study, EST 11j15	Data not shown	N/A
KH.C7.753	TG, thyroglobulin-1	KH.C7.753	Diffuse staining, stronger in notochord and in the trunk	Notochord	This Study, EST 73e.01	Fig. 4E	Thyroglobulin
KH.C4.191		SO1B1; SO1B3; SO1C1; SO2B1; SO3A1	Unclear signal	No expression/ Unclear	This Study, EST 94L12	Data not shown	Transmembrane transporter
KH.C1.158		GSH1	Semi-ubiquitous, including transient notochord; stronger in mesenchyme	Notochord	This Study, EST 26j01	Fig. 4J	Glutamate-cysteine ligase activity
KH.C3.304		RGS4; RGS5; RGS8	Notochord at late neurula	Notochord	This Study, EST 103j23	Fig. 4B	GTPase activator activity
KH.C1.426		RN103	Tail muscle	Not consistent	This Study, EST 70k01	Data not shown	Zinc ion binding
KH.L22.56	A4GALT, 4-Alpha-Galactosyltransferase	KH.L22.56	Epidermis, presumptive palps	Epidermis	This Study, EST 92L06	Fig. 4O	N/A
KH.C1.973		KH.C1.973	Ubiquitous, including notochord, stronger in CNS and part of the epidermis	Notochord	This Study, EST 103j24	Fig. 4L	N/A
KH.S638.1		KH.S638.1	Mesenchyme	Not consistent	This Study, EST 39n05	Data not shown	N/A
KH.C14.386	C6/7, complement component 6	CO6; CO8A; CO9	Mesenchyme; hemocytes of juveniles	Not consistent	This Study, EST 69O17; Ogasawara et al. (2006)	Data not shown	Membrane attack complex
KH.C11.196		LARP6	Strong epidermis	Epidermis	This Study, EST 25p09	Fig. 4N	RNA binding
KH.C2.411	CUTL-29	KH.C2.411	Epidermis, transient notochord	Notochord	This Study, EST 33e.07	Fig. 4C	N/A
KH.C14.206		BDH2; DCXR; DHB14	No expression	No expression	This Study, EST 69L21	Data not shown	Oxidoreductase activity
KH.L170.59		DNJB1; DNJB4; DNJB5	Semi-ubiquitous, stronger in CNS, mesenchyme and palps at the late tailbud stage	CNS	This Study, EST 92N23	Data not shown	Unfolded protein binding
KH.L106.8		GDIR1	Semi-ubiquitous, stronger in notochord and transiently expressed in notochord precursors	Notochord	This Study, EST 43m04	Fig. 4I and data not shown	Rho GDP-dissociation inhibitor activity
KH.S852.5	TRP-4	ANKUB	Very faint mesenchyme	Not consistent	This Study, EST 37o02	Data not shown	Ankyrin Repeat and Ubiquitin Domain

(continued on next page)

Table 2 *(continued)*

KH gene model	Alternative/former Gene Name(s)	Latest Gene Name	Expression	Classified as:	Reference	Figure	Gene Ontology
KH.C9.842	LINGO1/2/3/4	LIGO1; LIGO2; LIGO3	Diffuse staining, stronger in sensory vesicle	CNS	This Study, EST 08a19	Data not shown	Integral to membrane, positive regulation of synapse assembly
KH.S404.8		KH.S404.8	No expression	No expression	This Study, EST 69L04	Data not shown	N/A
KH.C7.26		KH.C7.26	Diffuse staining in the tail, including notochord	Notochord	This Study EST 43a17	Fig. 4G	N/A
KH.C14.36		KH.C14.36	Epidermis, predominantly ventral midline	Epidermis	This Study EST 32c05	Data not shown	N/A
KH.L18.49	NAALAD12	KH.L18.49	Notochord and diffuse staining in the trunk; stomach of juveniles	Notochord	This Study EST 03h24 Ogasawara et al. (2002)	Fig. 4F	N/A
KH.L13.2		KH.L13.2	Notochord	Notochord	Our unpublished results	Data not shown	Basement membrane
KH.C5.124	CLDN16/17/19	KH.C5.124	Notochord	Notochord	This Study, EST 33g05 also in Aniseed database, Brozovic et al. (2016)	Fig. 5C	Bicellular tight junction

evolutionarily conserved putative lysyl-oxidase, which in the vertebrate notochord reinforces the ECM by cross-linking collagen and elastin (Kugler et al., 2008) and KH.L13.2 is a putative component of basement membranes; we tentatively classified as a basement membrane/ECM component the predicted protein of KH.C7.753, which contains thyroglobulin-like repeats and has weak sequence homology with nidogen-like proteins. MP1 a serine-type endopeptidase, Beta4GalT is a mediator of carbohydrate metabolism and GSH1 a putative glutamate-cysteine ligase (grouped as 'enzymes' in Fig. 4R).

3.5. Positioning Bhlh-tun1 within the Ci-Bra-downstream notochord gene regulatory network

We cross-referenced the list of 21 Bhlh-tun1 notochord target genes with the available lists of Ci-Bra-downstream notochord genes (Takahashi et al., 1999; Hotta et al., 2000, 2008; Kugler et al., 2008; Reeves et al., 2017; our unpublished results) and with the genes targeted by Tbx2/3, a transcription factor that is part of the Ci-Bra-downstream notochord GRN (José-Edwards et al., 2013), and determined that 16/21 Bhlh-tun1 targets (76.2%) were also under the control of Ci-Bra, and that two of these 16 genes were controlled by both Ci-Bra and Tbx2/3 (Table 3). Of note, expression of two of the putative Bhlh-tun1 target genes identified in this study, AGRD1, (KH.C9.832) and MLKL (KH.C4.411), had been tested in Ci-Bra$^{-/-}$ embryos and had been found to be undetectable by WMISH, while strongly expressed in wild-type control embryos (Chiba et al., 2009). As a next step, we sought to validate the results of the microarray screens, using either WMISH or qRT-PCR on embryos carrying the *FoxA.a > Bhlh-tun1* transgene. The *FoxA.a > Bhlh-tun1* construct (Fig. 3C,C′) efficiently mis-expressed Bhlh-tun1 in CNS and endoderm, as shown by WMISH (Fig. 5A,B). We assayed the expression of genes expressed either predominantly or specifically in the notochord by WMISH, and we found genes that are highly responsive to the mis-expression of Bhlh-tun1. One of these genes, Claudin16/17/19 (Fig. 5C,D), encodes for a Claudin that was originally annotated as Claudin16-like and subsequently as Claudin16/17/19 to equally relate its sequence to members of Claudin families 16, 17 and 19 (Lal-Nag and Morin, 2009); tBLASTN searches indicated sequence identities also with members of the Claudin families 1 and 15. This gene is predominantly expressed in the *Ciona* notochord at the tailbud stages, and a faint hybridization signal can be observed also in mesenchyme and part of the sensory vesicle (Fig. 5C and Aniseed database; Brozovic et al., 2016). In embryos electroporated with the *FoxA.a > Bhlh-tun1* plasmid, ectopic expression is detected in the CNS, particularly in part of the nerve cord, and a stronger signal is observed in the notochord (Fig. 5D). In accordance with the results of the microarray screens and WMISH experiments, qRT-PCR on whole embryos indicates that this gene is up-regulated as a consequence of Bhlh-tun1 overexpression (Fig. 5E). To further investigate the relationship between Claudin16/17/19 and Bhlh-tun1, we scanned the genomic sequence located 5′ of this coding region and identified a short sequence interval containing a cluster of three E-boxes; when tested *in vivo*, a 300-bp genomic fragment containing the three E-boxes was able to recapitulate the notochord staining observed by WMISH (Fig. 5F). A few genes expressed predominantly in the notochord but also expressed at low levels in additional tissues, such as Lox1 (Kugler et al., 2008), S22A1/4/5 (Fig. 4K), and KH.C1.973 (Fig. 4L), did not provide clear results in WMISH and/or in qRT-PCR experiments, likely because of their diffuse expression in the majority of embryonic tissues. We carried out validation experiments using either WMISH or qRT-PCR or both for other putative Bhlh-tun1-downstream notochord genes with more localized expression patterns (Fig. 6), and verified the up-regulation of additional notochord genes in *FoxA.a > Bhlh-tun1* transgenic embryos, including SWP70 (Fig. 6A,B), AGRD1 (Fig. 6C,D), TBC3C/D (KH.C2.208, Table 3; Fig. 6E, graph on the left), Lhx3/4/5 (KH.S215.4; Imai et al., 2004; Fig. 6E, graph on the right), and

Table 3
Bhlh-tun1 target genes expressed in the developing notochord.

KH gene model	Alternative/former Gene Name(s)	Latest Gene Name	Expression	Reference	Figure	Gene Ontology	Classified in Fig. 4R as:	Additional upstream notochord regulators
KH.S1032.2	SHROOM/3	SHRM2; SHRM3; SHRM4	Ubiquitous, slightly stronger in notochord and mesenchyme	**This Study, EST 16f20**	Fig. 4H	Actin binding	Cell-shape	Ci-Bra*
KH.C4.411	MLKL	MLKL; RIPK1; TESK2	Notochord-specific	Jose'-Edwards et al. (2013)		Protein kinase, transmembrane cation channel	Transmembrane	Ci-Bra* and Tbx2/3**
KH.C9.832	GPR133	AGRD1; AGRL2; LPHN3	Diffuse signal in the trunk, stronger in notochord	**This Study, EST 27F07**	Fig. 4D	Transmembrane signaling receptor activity	Transmembrane	Ci-Bra*
KH.C8.476	Ci-Lox1	LOXL2; LOXL3; LOXL4	Notochord	Kugler et al. (2008)		Scavenger receptor activity; protein-lysine 6-oxidase activity	ECM	Ci-Bra*
KH.C2.377	MP1	KLK5; PRSS8; TMPS9	Diffuse staining, including epidermis and notochord	**This Study, EST 25f15**	Fig. 4M	Serine-type endopeptidase	Enzyme	Ci-Bra*
KH.C2.91	TPO1/2/3 (Ci-Organic cation/carnitine transporter 2 like	S22A1; S22A4; S22A5	Ubiquitous, including notochord precursors, stronger in CNS	**This Study, EST 70b01**	Fig. 4K	Transmembrane transporter	Transmembrane	Ci-Bra***
KH.C5.124	CLDN16/17/19	KH.C5.124	Notochord	**This Study, EST 33g05** also in Aniseed database (Brozovic et al., 2016)	Fig. 5	Bicellular tight junction	Transmembrane	Ci-Bra***
KH.C7.753	TG, thyroglobulin-1	KH.C7.753	Diffuse staining, stronger in notochord and in the trunk	**This Study, EST 73e.01**	Fig. 4E	Basement membrane (tentative)	ECM	Ci-Bra*
KH.C7.26		KH.C7.26	Diffuse staining in the tail, including notochord	**This Study EST 43a17**	Fig. 4G	N/A	N/A	Ci-Bra*
KH.C2.208	USP6NL	TBC3C; TBC3D; US6NL	Notochord	Reeves et al. (2017)		GTPase activator activity	Cell-shape	Ci-Bra*
KH.C1.158		GSH1	Semi-ubiquitous, including transient notochord; stronger in mesenchyme	**This Study, EST 26j01**	Fig. 4J	Glutamate-cysteine ligase activity	Enzyme	
KH.C3.304		RGS4; RGS5; RGS8	Notochord at late neurula	**This Study, EST 103j23**	Fig. 4B	GTPase activator activity	Cell-shape	Ci-Bra*
KH.C4.326		SWP70	Notochord, epidermis, mesenchyme, nervous system	Satou et al. (2001)		Guanine nucleotide exchange factor, regulator of cytoskeletal rearrangement	Cell-shape	Ci-Bra*
KH.C1.973		KH.C1.973	Ubiquitous, stronger in CNS and part of the epidermis	**This Study, EST 103j24**	Fig. 4L	N/A	N/A	
KH.S215.4	LHX3/4	LHX3; LHX4; LHX5	Endoderm, notochord and a few muscle precursors neural folds; anterior sensory vesicle, visceral ganglion	Imai et al. (2004); Kobayashi et al. (2010)		Transcription factor	Transcription factor	Ci-Bra*
KH.S655.4	Ci-META6-like	KH.S655.4	Notochord; endostyle of juveniles	Jose'-Edwards et al. (2013); Ogasawara et al. (2002).	Fig. 7A	N/A	N/A	Ci-Bra* and Tbx2/3**
KH.L13.2		KH.L13.2	Notochord	Our unpublished results		Basement membrane	ECM	Ci-Bra*
KH.C2.411	CUTL-29	KH.C2.411	Mostly epidermis, transient notochord	**This Study, EST 33e.07**	Fig. 4C	N/A	N/A	

(continued on next page)

Table 3 *(continued)*

KH gene model	Alternative/former Gene Name(s)	Latest Gene Name	Expression	Reference	Figure	Gene Ontology	Classified in Fig. 4R as:	Additional upstream notochord regulators
KH.L106.8		GDIR1	Semi-ubiquitous, stronger in notochord and transiently expressed in notochord precursors	**This Study, EST 43m04**	Fig. 4I and data not shown	Rho GDP-dissociation inhibitor activity	Cell-shape	
KH.L18.49	NAALADL2	KH.L18.49	Notochord and diffuse staining in the trunk; stomach of juveniles	**This Study EST 03h24** Ogasawara et al. (2002)	Fig. 4F	N/A	N/A	
KH.C11.44	Beta-4-galT	B4GT1; B4GT2; B4GT3	Notochord	Hotta et al. (2000)		Galactosyltransferase activity	Enzyme	Ci-Bra[§*]

[§] Hotta et al., 2000.
[*] Kubo et al., 2010.
[**] José-Edwards et al., 2013.
[***] Our unpublished results.

KH.L13.2 (Fig. 6F, graph on the left). We also determined that expression of Beta4GalT is down-regulated by the over-expression of Bhlh-tun1 in late tailbuds (Fig. 6F, graph on the right), while no significant effect was observed on the expression of this gene in early tailbuds (data not shown). Also for other notochord genes, qRT-PCR experiments indicated that the effect of Bhlh-tun1 over-expression was in most cases stage-dependent, and in some instances the effect seemed to vary between the two stages at which the qRT-PCR experiments and the microarray experiments were performed (data not shown). Using WMISH, we verified that the overexpression of Bhlh-tun1 can also down-regulate expression of additional notochord genes such as META6-like (Fig. 7A), which in *FoxA.a > Bhlh-tun1* transgenic embryos is visibly down-regulated in notochord cells, while it remains steadily expressed in mesenchyme and is only marginally affected in CNS (Fig. 7B). We also tested the expression of epidermal genes targeted by Bhlh-tun1 (Table 2; summarized in Fig. 4Q). Microarray results indicated that Achaete-scute a-like 2 (KH.L9.13) is down-regulated in *FoxA.a > Bhlh-tun1* transgenic embryos, in agreement with the results obtained upon overexpression of Bhlh-tun1 in the midline (Roure and Darras, 2016). Similarly, the results of the microarray screens suggested that another epidermal gene newly identified in this study, *LARP6* (KH.C11.196) (Fig. 4N), is down-regulated in response to the overexpression of Bhlh-tun1; this result was confirmed by WMISH (Fig. 7C,D). A summary of the main results of this study and a working model for the position and functions of Bhlh-tun1 within the Ci-Bra-downstream notochord GRN are presented in Fig. 8.

4. Discussion

bHLH transcription factors participate in an array of developmental and morphogenetic processes in both animals and plants, and have been reported to regulate the expression of genes responsible for the assembly and stability of the cytoskeleton, in particular through the regulation of small GTPases (Ge et al., 2006). The compact and rarely redundant genome of the simple chordate *Ciona robusta* contains several readily recognizable transcription factor genes, which are often evolutionarily conserved orthologs of transcriptional regulators found in vertebrates (Dehal et al., 2002). Bhlh-tun1 does not display clear relationships with vertebrate bHLH proteins; rather, the fact that it possesses orthologs in other solitary ascidians, such as *Ciona savignyi*, *Phallusia mammillata* and *Phallusia fumigata*, and in the colonial ascidian *Botryllus schlosseri* (Aniseed database; Prünster et al., 2018), indicates that it is a tunicate-specific transcription factor. Previous studies had focused on its roles in midline formation (Roure and Darras, 2016) and in the development of the musculature of oral and atrial siphons after metamorphosis (Razy-Krajka et al., 2014; Tolkin and Christiaen, 2016). In this study, we investigated the role of this transcription factor in the developing *Ciona* notochord, its transcriptional regulation, binding properties, and target genes. Our results position *Bhlh-tun1* downstream of Ci-Bra, FoxA.a, and an early homodomain-containing activator, and suggest that Bhlh-tun1, in turn, can modulate the expression of Ci-Bra-downstream genes involved in the acquisition of cell-shape, in the maintenance of the characteristic rod-like shape of the notochord, and in the early stages of tubulogenesis.

4.1. Control of Bhlh-tun1 transcription in the notochord

Based upon its robust notochord expression and the timing of its onset of expression, we hypothesized that *Bhlh-tun1* transcription might be directly controlled by Ci-Bra. Indeed, we found that Bhlh-tun1 is ectopically expressed in embryos misexpressing Ci-Bra and is specifically down-regulated in the notochord of embryos lacking Ci-Bra function, and we isolated a 1.7-kb notochord CRM from the *Bhlh-tun1* genomic locus that responds to Ci-Bra misexpression in the same way

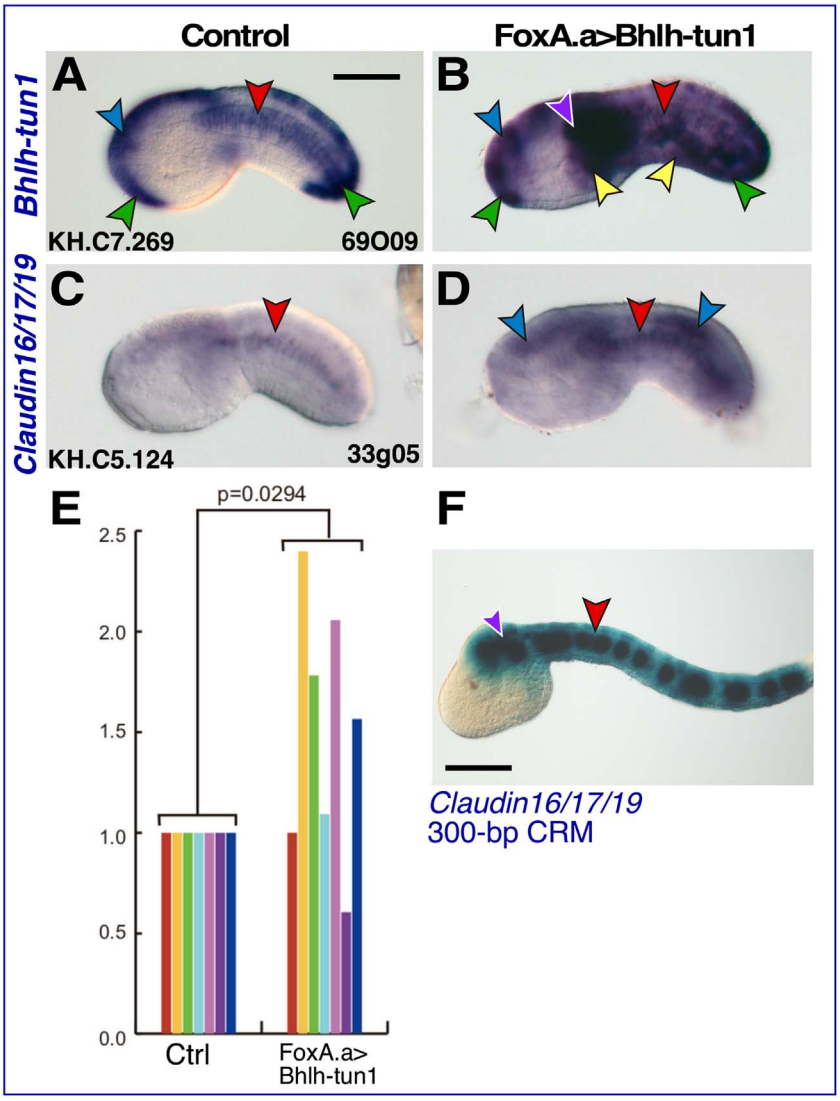

Fig. 5. Up-regulation of Claudin16/17/19 in embryos over-expressing Bhlh-tun1. (A-D) WMISH of control (A,C) and transgenic (B,D) *Ciona* embryos, performed using the digoxigenin-labeled antisense RNA probes synthesized using as templates the EST clones reported in the bottom right corner of panels A and C. The current gene name is indicated on the left side of each row. Gene models are indicated in the left bottom corner of panels A and C. Arrowheads are color-coded as in Fig. 1; yellow arrowheads indicate endodermal cells. (E) Graph showing the results of qRT-PCR experiments aimed at validating the over-expression detected by WMISH, performed at the same stage (stage 19/early tailbud stage 1; see Methods). Details of the experimental results are listed in Table S1, oligonucleotide sequences can be found in Table S2. p, p-value; ctrl, control (wild-type) embryos. (F) Late-tailbud II embryo electroporated at the 1-cell stage with a 300-bp fragment identified in the 5′-flanking region of *Claudin16/17/19*, containing a cluster of three E-boxes. The embryo was stained using X-Gal for about 4 h at 37 °C. Scale bars indicate approximately 100 μm in A and 50 μm in F.

as *Bhlh-tun1*. A thorough truncation/mutation analysis of the 1.7-kb CRM identified a 144-bp region that directed reproducible notochord staining *in vivo* and contained a cluster of three putative Ci-Bra binding sites and two binding sites for Fox proteins. Differently from our previous findings for other notochord CRMs (Passamaneck et al., 2009; Katikala et al., 2013; José-Edwards et al., 2015), the simultaneous mutation of these sites reduced notochord staining, but was not sufficient to abolish it. Furthermore, even though *Bhlh-tun1* is present in both *Ciona robusta* and *Ciona savignyi* (Aniseed database https://www.aniseed.cnrs.fr; Brozovic et al., 2016), the notochord CRM that we have identified is poorly conserved, and the interspecific sequence alignments display only limited and scattered sequence identity (data not shown), which did not assist in our search for the minimal sequences required for notochord activity of this non-conserved CRM. For this reason, we further truncated the 144-bp CRM and identified the 58-bp region that still elicited reproducible notochord staining, and a 49-bp region that had no activity in the notochord. Serial mutations of the 9 bp that differed between these regions indicated that an ATTA minimal homeodomain binding site was responsible for the notochord activity of the 58-bp region. We had previously reported that an ATTA core sequence is required also for the function of the notochord CRM of *Ci-ACL* (Katikala et al., 2013); we have also described the requirement of adjacent homeodomain and Fox binding sites for the function of another notochord CRM, Ci-CRM112 (José-Edwards et al., 2015). An early-onset homeodomain activator, which is presumably expressed before early gastrulation, could be working cooperatively with FoxA.a, an early-onset pioneer chromatin-opening factor, and thus render the CRM accessible to binding by Ci-Bra. We searched the published expression patterns for homeodomain proteins expressed in the notochord during the stages preceding the reported appearance of *Bhlh-tun1* transcripts, and found two possible candidate homeodomain activators, Mnx and Lhx3/4/5 (KH.L128.12 and KH.S215.4, respectively; Imai et al., 2004).

In addition to the notochord CRM, within the *Bhlh-tun1* locus we have also identified a 995-bp epidermal CRM, which might be employed to further clarifying the regulation of *Bhlh-tun1* expression in epidermal lineages.

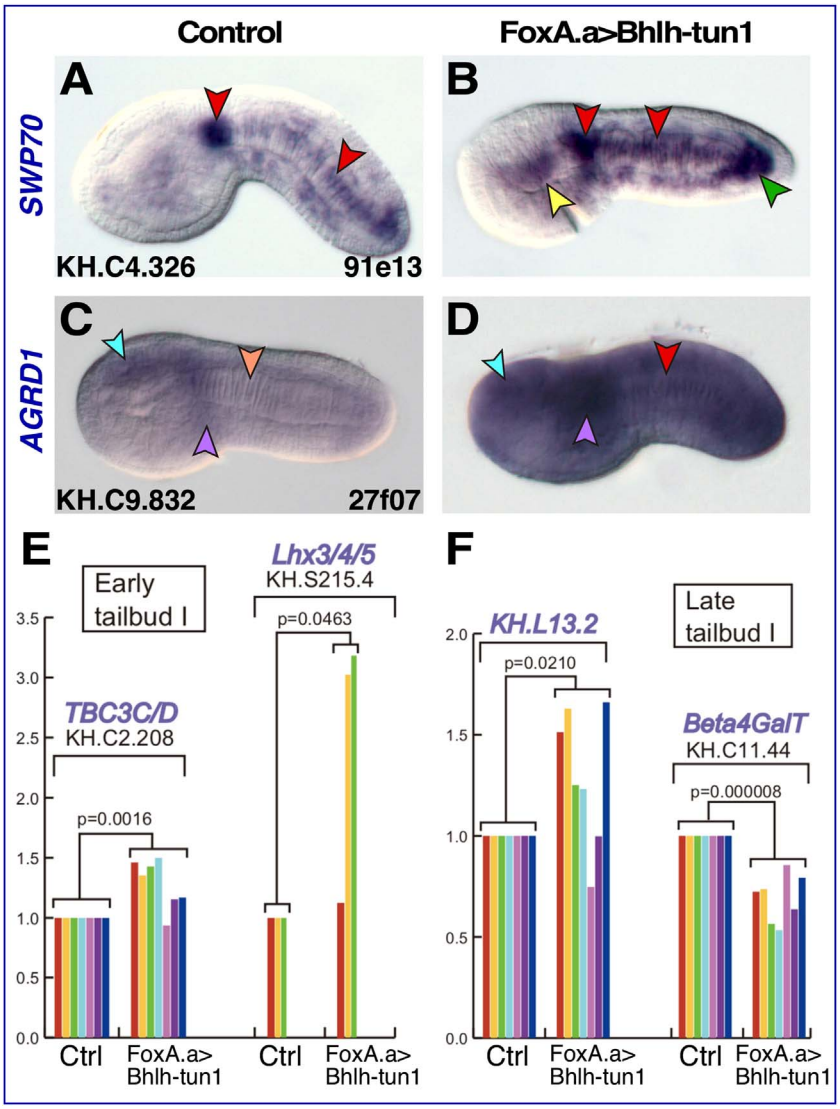

Fig. 6. Validation of additional Bhlh-tun1 early and late target genes expressed in the developing notochord. (A-D) WMISH of control (A,C) and transgenic (B,D) *Ciona* embryos, performed using the digoxigenin-labeled antisense RNA probes synthesized using as templates the EST clones reported in the bottom right corner of panels A and C. The current gene name is indicated on the left side of each row. Gene models are indicated in the left bottom corner of panels A and C. Arrowheads are color-coded as in Fig. 1; yellow arrowheads indicate endodermal cells. The light pink arrowhead in C indicates weak notochord staining (see also Fig. 4D). (E,F) Graphs showing the results of qRT-PCR experiments aimed at validating the over-expression detected by WMISH, performed at the same stage as panels A-D (stage 19/early tailbud stage I; panel E), or at the stage 23/late tailbud I (F). p, p-value; ctrl, control (wild-type) embryos. Details of the experimental results are listed in Table S1, oligonucleotide sequences can be found in Table S2.

4.2. Bhlh-tun1 as an intermediary of Ci-Bra in notochord development

Information on the identity and specific roles of transcriptional intermediaries of Brachyury in notochord development is still fragmentary in most chordates. The dependence of *Bhlh-tun1* expression upon Ci-Bra suggested that in *Ciona* Bhlh-tun1 might function as one of its intermediaries in the activation of middle- or late-onset notochord genes. In support of this hypothesis, most of the Bhlh-tun1-downstream genes were previously reported to be downstream of Ci-Bra (Takahashi et al., 1999; Hotta et al., 2000; Kugler et al., 2008; Kubo et al., 2010), and two of these genes are also targets of Tbx2/3, another transcriptional intermediary of Ci-Bra (José-Edwards et al., 2013). The notochord phenotype observed in transgenic embryos overexpressing Bhlh-tun1 suggests its involvement in cell-shape changes and in intercalation movements, and preliminary shRNA-mediated knock-down experiments tentatively confirmed these findings (data not shown). We attempted to generate loss-of-function phenotypes using both morpholino oligonucleotide-mediated knock-downs and CRISPR/Cas9-mediated genomic editing, but we did not obtain specific results. The results of this study suggest that Bhlh-tun1 increases transcription of SWP70/SWAP70, an evolutionarily conserved guanine-exchange factor that stimulates actin polymerization and cytoskeletal rearrangements (Shinohara et al., 2002). Other notochord genes up-regulated by the overexpression of Bhlh-tun1 include *AGRD1* (adhesion G-protein coupled receptor D1), which encodes a 7-pass G-protein coupled transmembrane receptor that in other systems mediates the interactions between cells and ECM (Bohnekamp and Schöneberg, 2011), *TBC3C/D*, one of the GTPase activators identified in this study, and KH.L13.2. This latter gene encodes a predicted component of the basement membrane and is associated with a notochord CRM that has been identified and fully characterized in our laboratory, Ci-CRM9. This CRM is dependent upon a single Ci-Bra binding site, yet it contains three E-boxes within its neighboring sequence, which might be used by Bhlh-tun1 to finely modulate the levels of its expression in the notochord (José-Edwards et al., 2015). This configuration is also reminiscent of the arrangement that we found in the Claudin16/17/19 notochord CRM, whereby a

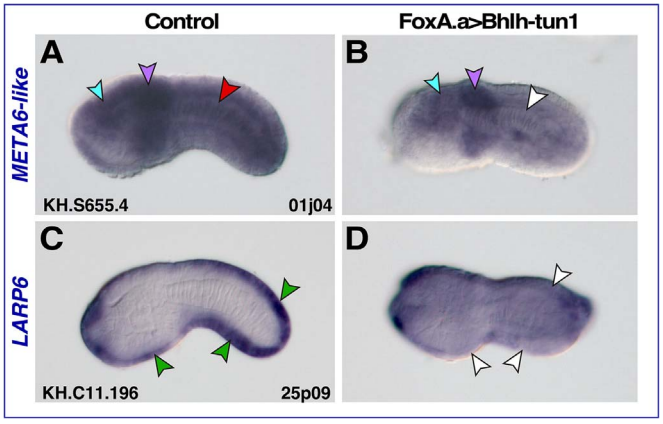

Fig. 7. Genes down-regulated by the over-expression of Bhlh-tun1. (A–D) WMISH of control (A,C) and transgenic (B,D) *Ciona* embryos, performed using the digoxigenin-labeled antisense RNA probes synthesized using as templates the EST clones reported in the bottom right corner of panels A and C. The current gene name is indicated on the left side of each row. Gene models are indicated in the left bottom corner of panels A and C. Arrowheads are color-coded as in Fig. 1.

cluster of three E-boxes is part of a 300-bp CRM with strong notochord activity. Claudin16/17/19 attracted our attention because it is a member of a family of 12 predicted *Ciona* claudins (Dehal et al., 2002). Claudins are major components of tight junctions, and in turn, tight junctions are required for tubulogenesis of the *Ciona* notochord, i.e., for its transformation from an epithelial sheet of 40 cells into a hollow tube that will be used by the larva as a hydrostatic skeleton for its swimming movements (Denker et al., 2013). In particular, tight junctions replace adherens junctions at the apical-lateral interface between notochord cells, an event that is necessary for the formation of extracellular pockets, which will eventually coalesce and form a continuous cavity in the center of the notochord (Dong et al., 2009; Denker et al., 2013). We noticed that Claudin16/17/19 transcripts become detectable in the nuclei of notochord cells around the early tailbud II stage, and that the notochord CRM that we have identified becomes active in the notochord only about one or two cell divisions before this stage (data not shown). These observations are in agreement with the timing of the appearance of tight junctions in the notochord. The presence of clustered E-box sequences within this region guided us in the identification of this regulatory module, and suggests that Bhlh-tun1 might contribute to the activity of this CRM and influence expression of this claudin through it. The predicted roles of these Ci-Bra/Bhlh-tun1-downstream notochord genes are consistent with the function in cell-shape changes that could be predicted for Bhlh-tun1 on the basis of the notochord phenotype induced by its overexpression. The up-regulation of *Lhx3/4/5* is of interest, because it is, together with Mnx, an homeodomain-containing transcription factor and a candidate activator of *Bhlh-tun1*, as suggested by the analysis of the *Bhlh-tun1* notochord CRM. However, Lhx3/4/5 is only expressed for a short amount of time in notochord precursors, and rapidly switches to endoderm and muscle precursors (Imai et al., 2004). Even though overexpression of Bhlh-tun1 is able to cause ectopic expression of *Lhx3/4/5*, the expression pattern of this gene in wild-type embryos suggests that this positive feedback of Bhlh-tun1 on *Lhx3/4/5* might be prevented during normal development by additional regulatory mechanisms.

Another relevant notochord target gene shared by Ci-Bra and Bhlh-tun1 is *Beta4GalT*, which is activated indirectly by Ci-Bra through a Myb-like transcriptional intermediary (Katikala et al., 2013); the present study suggests that in late stages of notochord development Bhlh-tun1 down-regulates *Beta4GalT*, thus counteracting Ci-Bra. Overexpression of Bhlh-tun1 in the notochord also induces down-regulation of *META6-like*, a gene that is activated by Tbx2/3 (José-Edwards et al., 2013), appears to be specific to the genus *Ciona* and encodes for a protein that does not contain recognizable conserved domains, whose function in notochord formation is unknown. The regulatory dynamic is different in the case of another Ci-Bra-down-

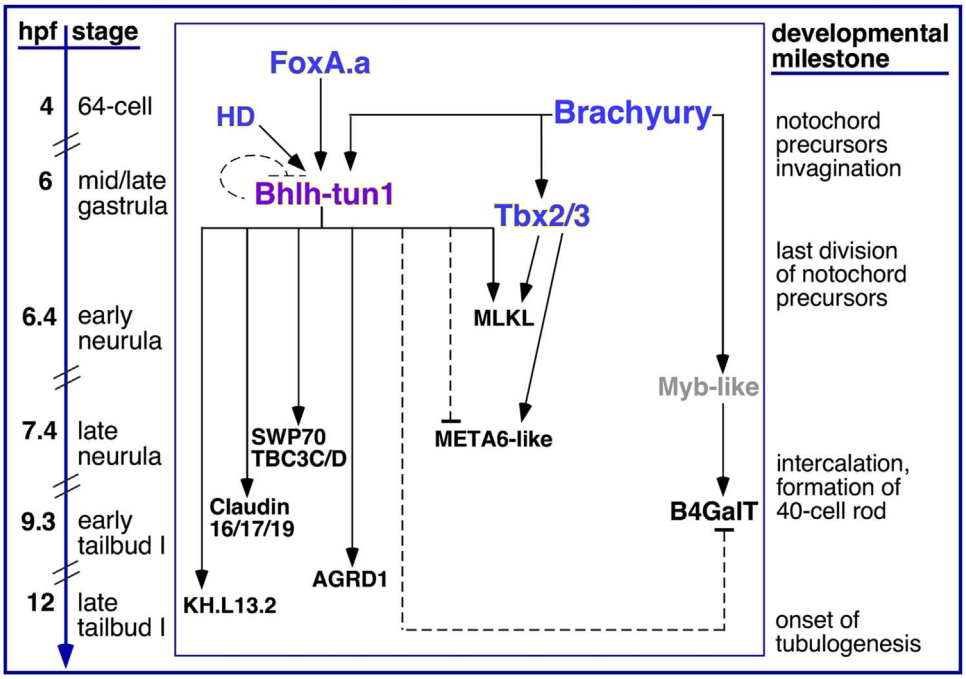

Fig. 8. Position of Bhlh-tun1 and a few of its notochord target genes within the Ci-Bra-downstream gene regulatory network. Left side: main stages of *Ciona* development that precede lumen formation (tubulogenesis) are shown for reference. Right side: a few of the main developmental milestones that punctuate notochord morphogenesis are listed. Hpf: hours post-fertilization. Central panel: a simplified view of the branch of the *Ciona* notochord GRN controlled by Bhlh-tun1. Additional transcription factors that compose the *Ciona* notochord GRN can be found elsewhere (Imai et al., 2006; Kugler et al., 2008; José-Edwards et al., 2011). Names of transcription factors are colored in blue (Bhlh-tun1 in violet), structural genes or enzymes in black. A Myb-like transcription factor that activates expression of Beta4GalT (B4GalT) is colored in grey (Katikala et al., 2013 and our unpublished results). Arrows symbolize (direct/indirect) activation of gene expression. Dashed lines with flat ends indicate (direct/indirect) down-regulation of gene expression, the extent of which remains to be determined. HD, homeodomain transcription factor that contributes to activate expression of Bhlh-tun1, presumed on the basis of the notochord CRM analysis (Fig. 2).

stream notochord gene, *MLKL*, which has been shown to form cation channels and induce membrane depolarization (Xia et al., 2016); in addition to being reportedly under the control of Ci-Bra, this gene seems to be up-regulated by both Bhlh-tun1 and Tbx2/3 (José-Edwards et al., 2013). Together, these results indicate that Bhlh-tun1 acts downstream of Ci-Bra in the notochord GRN to modulate gene expression either positively or negatively, possibly in a stage-specific fashion. It remains to be ascertained in each specific case whether these regulatory interactions are achieved directly or indirectly.

4.3. Multiple functions of Bhlh-tun1 in different tissues and developmental stages

Considering that Bhlh-tun1 is a very short bHLH protein, consisting almost exclusively of a DNA-binding domain and lacking an evident transactivation domain, it is conceivable that it might heterodimerize with different tissue-specific partners in order to function in distinct structures and that, even within a specific cell-type, Bhlh-tun1 might interact with stage-specific partners and modify its behavior accordingly. One such partner could be another bHLH transcription factor expressed in the developing *Ciona* notochord, such as Ci-ARNT, which is also activated by Ci-Bra (Hotta et al., 2008). ARNT bHLH factors have been shown to heterodimerize and induce transcriptional repression in different model systems (e.g. Sakurai et al., 2017). Moreover, Bhlh-tun1 might be able to activate yet uncharacterized stage-specific repressors or activators and exert its function indirectly.

In addition to shedding light on a group of *Ciona* notochord genes, most of which were previously uncharacterized, this study has detected a number of epidermal genes, such as *LARP6*, that are responsive to the overexpression of Bhlh-tun1 driven by the *FoxA.a* promoter region. Expression of these epidermal genes might have been induced by the ectopic expression of Bhlh-tun1 in epidermis, caused by the leaky activity of the 3-kb *FoxA.a* promoter region in this tissue. Previous studies have shown that the overexpression of Bhlh-tun1 causes a down-regulation of the expression of *Achaete-scute a-like 2* (KH.L9.13) (Roure and Darras, 2016). The results of our microarray screen are in agreement with this regulatory scenario, as *Achaete-scute a-like 2* expression is reduced in embryos overexpressing Bhlh-tun1 (data not shown). Similarly, we demonstrated the down-regulation of *LARP6* caused by the overexpression of Bhlh-tun1. These results suggest that in epidermal lineages Bhlh-tun1 might prevalently act, either directly or indirectly, as a negative modulator of gene expression.

In conclusion, Bhlh-tun1 is a tunicate-specific transcription factor that before metamorphosis participates in the GRNs responsible for cell-fate acquisition in the neurogenic ectoderm midline (Roure and Darras, 2016) and after metamorphosis is a Notch-downstream marker of muscle stem cells involved in the development of the siphon musculature (Razy-Krajka et al., 2014; Tolkin and Christiaen, 2016). Here we have shown a role for this transcriptional regulator in the axial mesoderm, where it controls cell-shape changes, intercalation, proper extension of the notochord, and possibly the initial phases of the formation of its lumen. It seems likely that this transcriptional regulator has been incorporated into the Brachyury-downstream GRN after the branching of tunicates from the main chordate lineage, and thus represents a divergent mechanism of control of notochord gene expression.

Acknowledgments

We acknowledge Dr. Nori Satoh and members of his lab (Okinawa Institute of Science and Technology) for the microarray screens. We thank Drs. William Smith and Shota Chiba (University of California, Santa Barbara) for the mutant Ci-Bra embryos. We are grateful to Mr. Joseph Afzali and Ms. Irina Pyatigorskaya for technical help, and to Drs. Sébastien Darras and Florian Razy-Krajka for insightful discussion. This work was supported by the National Institutes of Health/National Institute of General Medical Sciences (NIH/NIGMS R01GM100466) and by start-up funds from NYU College of Dentistry to ADG.

Appendix A. Supplementary material

Supplementary data associated with this article can be found in the online version at doi:10.1016/j.ydbio.2019.01.002.

References

Azumi, K., Takahashi, H., Miki, Y., Fujie, M., Usami, T., Ishikawa, H., Kitayama, A., Satou, Y., Ueno, N., Satoh, N., 2003. Construction of a cDNA microarray derived from the ascidian *Ciona intestinalis*. Zool. Sci. 20, 1223–1229.

Bohnekamp, J., Schöneberg, T., 2011. Cell adhesion receptor GPR133 couples to Gs protein. J. Biol. Chem. 286, 41912–41916.

Brozovic, M., Martin, C., Dantec, C., Dauga, D., Mendez, M., Simion, P., Percher, M., Laporte, B., Scornavacca, C., Di Gregorio, A., et al., 2016. ANISEED 2015: a digital framework for the comparative developmental biology of ascidians. Nucleic Acids Res. 44 (D1), D808–D818.

Chiba, S., Jiang, D., Satoh, N., Smith, W.C., 2009. *Brachyury* null mutant-induced defects in juvenile ascidian endodermal organs. Development 136, 35–39.

Corbo, J.C., Levine, M., Zeller, R.W., 1997. Characterization of a notochord-specific enhancer from the *Brachyury* promoter region of the ascidian, *Ciona intestinalis*. Development 124, 589–602.

Dehal, P., Satou, Y., Campbell, R.K., Chapman, J., Degnan, B., De Tomaso, A., Davidson, B., Di Gregorio, A., Gelpke, M., Goodstein, D.M., et al., 2002. The draft genome of *Ciona intestinalis*: insights into chordate and vertebrate origins. Science 298, 2157–2167.

Denker, E., Bocina, I., Jiang, D., 2013. Tubulogenesis in a simple cell cord requires the formation of bi-apical cells through two discrete Par domains. Development 140, 2985–2996.

Dong, B., Horie, T., Denker, E., Kusakabe, T., Tsuda, M., Smith, W.C., Jiang, D., 2009. Tube formation by complex cellular processes in *Ciona intestinalis* notochord. Dev. Biol. 330, 237–249.

Di Gregorio, A., Levine, M., 1999. Regulation of *Ci-tropomyosin-like*, a Brachyury target gene in the ascidian, *Ciona intestinalis*. Development 126, 5599–5609.

Di Gregorio, A., Corbo, J.C., Levine, M., 2001. The regulation of *forkhead/HNF-3beta* expression in the *Ciona* embryo. Dev. Biol. 229, 31–43.

Dunn, M.P., Di Gregorio, A., 2009. The evolutionarily conserved *leprecan* gene: its regulation by Brachyury and its role in the developing *Ciona* notochord. Dev. Biol. 328, 561–574.

Frohman, M.A., 1993. Rapid amplification of complementary DNA ends for generation of full-length complementary DNAs: thermal RACE. Methods Enzymol. 218, 340–356.

Fujiwara, S., Maeda, Y., Shin-I, T., Kohara, Y., Takatori, N., Satou, Y., Satoh, N., 2002. Gene expression profiles in *Ciona intestinalis* cleavage-stage embryos. Mech. Dev. 112, 115–127.

Ge, W., He, F., Kim, K.J., Blanchi, B., Coskun, V., Nguyen, L., Wu, X., Zhao, J., Heng, J.I., Martinowich, K., Tao, J., Wu, H., Castro, D., Sobeih, M.M., Corfas, G., Gleeson, J.G., Greenberg, M.E., Guillemot, F., Sun, Y.E., 2006. Coupling of cell migration with neurogenesis by proneural bHLH factors. Proc. Natl. Acad. Sci. USA 103 (5), 1319–1324.

Gilchrist, M.J., Sobral, D., Khoueiry, P., Daian, F., Laporte, B., Patrushev, I., Matsumoto, J., Dewar, K., Hastings, K.E., Satou, Y., Lemaire, P., Rothbächer, U., 2015. A pipeline for the systematic identification of non-redundant full-ORF cDNAs for polymorphic and evolutionary divergent genomes: application to the ascidian *Ciona intestinalis*. Dev. Biol. 404, 149–163.

Gyoja, F., 2017. Basic helix-loop-helix transcription factors in evolution: roles in development of mesoderm and neural tissues. Genesis 55 (9).

Hotta, K., Mitsuhara, K., Takahashi, H., Inaba, K., Oka, K., Gojobori, T., Ikeo, K., 2007. A web-based interactive developmental table for the ascidian *Ciona intestinalis*, including 3D real-image embryo reconstructions: i. From fertilized egg to hatching larva. Dev. Dyn. 236, 1790–1805.

Hotta, K., Takahashi, H., Asakura, T., Saitoh, B., Takatori, N., Satou, Y., Satoh, N., 2000. Characterization of Brachyury-downstream notochord genes in the *Ciona intestinalis* embryo. Dev. Biol. 224, 69–80.

Hotta, K., Takahashi, H., Satoh, N., Gojobori, T., 2008. Brachyury-downstream gene sets in a chordate, *Ciona intestinalis*: integrating notochord specification, morphogenesis and chordate evolution. Evol. Dev. 10, 37–51.

Hudson, C., Lemaire, P., 2001. Induction of anterior neural fates in the ascidian *Ciona intestinalis*. Mech. Dev. 100, 189–203.

Imai, K.S., Hino, K., Yagi, K., Satoh, N., Satou, Y., 2004. Gene expression profiles of transcription factors and signaling molecules in the ascidian embryo: towards a comprehensive understanding of gene networks. Development 131, 4047–4058.

Imai, K.S., Levine, M., Satoh, N., Satou, Y., 2006. Regulatory blueprint for a chordate embryo. Science 312, 1183–1187.

Jiang, D., Smith, W.C., 2007. Ascidian notochord morphogenesis. Dev. Dyn. 236, 1748–1757.

Jones, S., 2004. An overview of the basic helix-loop-helix proteins. Genome Biol. 5, 226.

José-Edwards, D.S., Kerner, P., Kugler, J.E., Deng, W., Jiang, D., Di Gregorio, A., 2011. The identification of transcription factors expressed in the notochord of *Ciona intestinalis* adds new potential players to the Brachyury gene regulatory network.

Dev. Dyn. 240, 1793–1805.
José-Edwards, D.S., Oda-Ishii, I., Nibu, Y., Di Gregorio, A., 2013. Tbx2/3 is an essential mediator within the Brachyury gene network during *Ciona* notochord development. Development 140, 2422–2433.
José-Edwards, D.S., Oda-Ishii, I., Kugler, J.E., Passamaneck, Y.J., Katikala, L., Nibu, Y., Di Gregorio, A., 2015. Brachyury, Foxa2 and the cis-Regulatory Origins of the Notochord. PLoS Genet. 11 (12), e1005730.
Katikala, L., Aihara, H., Passamaneck, Y.J., Gazdoiu, S., José-Edwards, D.S., Kugler, J.E., Oda-Ishii, I., Imai, J.H., Nibu, Y., Di Gregorio, A., 2013. Functional Brachyury binding sites establish a temporal read-out of gene expression in the *Ciona* notochord. PLoS Biol. 11 (10), e1001697.
Kispert, A., Koschorz, B., Herrmann, B.G., 1995. The T protein encoded by *Brachyury* is a tissue-specific transcription factor. EMBO J. 14, 4763–4772.
Kobayashi, M., Takatori, N., Nakajima, Y., Kumano, G., Nishida, H., Saiga, H., 2010. Spatial and temporal expression of two transcriptional isoforms of Lhx3, a LIM class homeobox gene, during embryogenesis of two phylogenetically remote ascidians, *Halocynthia roretzi* and *Ciona intestinalis*. Gene Expr. Patterns 10, 98–104.
Kubo, A., Suzuki, N., Yuan, X., Nakai, K., Satoh, N., Imai, K.S., Satou, Y., 2010. Genomic cis-regulatory networks in the early *Ciona intestinalis* embryo. Development 137, 1613–1623.
Kugler, J.E., Passamaneck, Y.J., Feldman, T.G., Regnier, T.W., Di Gregorio, A., 2008. Evolutionary conservation of vertebrate notochord genes in the ascidian *Ciona intestinalis*. Genesis 46, 697–710.
Kusakabe, T., Yoshida, R., Kawakami, I., Kusakabe, R., Mochizuki, Y., Yamada, L., Shin-I, T., Kohara, Y., Satoh, N., Tsuda, M., Satou, Y., 2002. Gene expression profiles in tadpole larvae of *Ciona intestinalis*. Dev. Biol. 242, 188–203.
Lal-Nag, M., Morin, P.J., 2009. The claudins. Genome Biol. 10 (8), 235.
Lemaire, P., Smith, W.C., Nishida, H., 2008. Ascidians and the plasticity of the chordate developmental program. Curr. Biol. 18 (14), R620–R631.
Miwata, K., Chiba, T., Horii, R., Yamada, L., Kubo, A., Miyamura, D., Satoh, N., Satou, Y., 2006. Systematic analysis of embryonic expression profiles of zinc finger genes in Ciona intestinalis. Dev. Biol. 292, 546–554.
Nagai, T., Ibata, K., Park, E.S., Kubota, M., Mikoshiba, K., Miyawaki, A., 2002. A variant of yellow fluorescent protein with fast and efficient maturation for cell-biological applications. Nat. Biotechnol. 20, 87–90.
Nibu, Y., José-Edwards, D.S., Di Gregorio, A., 2013. From notochord formation to hereditary chordoma: the many roles of Brachyury. Biomed. Res Int. 2013, 826435.
Oda-Ishii, I., Di Gregorio, A., 2007. Lineage-independent mosaic expression and regulation of the *Ciona multidom* gene in the ancestral notochord. Dev. Dyn. 236, 1806–1819.
Ogasawara, M., Nakazawa, N., Azumi, K., Yamabe, E., Satoh, N., Satake, M., 2006. Identification of thirty-four transcripts expressed specifically in hemocytes of Ciona intestinalis and their expression profiles throughout the life cycle. DNA Res. 13, 25–35.
Ogasawara, M., Sasaki, A., Metoki, H., Shin-i, T., Kohara, Y., Satoh, N., Satou, Y., 2002. Gene expression profiles in young adult Ciona intestinalis. Dev. Genes Evol. 212, 173–185.
Passamaneck, Y.J., Di Gregorio, A., 2005. *Ciona intestinalis*: chordate development made simple. Dev. Dyn. 233, 1–19.
Passamaneck, Y.J., Katikala, L., Perrone, L., Dunn, M.P., Oda-Ishii, I., Di Gregorio, A., 2009. Direct Activation of a Notochord *Cis*-regulatory Module by Brachyury and FoxA in the Ascidian *Ciona*. Development 136, 3679–3689.
Prünster, M.M., Ricci, L.F., Brown, F., Tiozzo, S., 2018. Modular co-option of cardiopharyngeal genes during non-embryonic myogenesis. bioRxiv. http://dx.doi.org/10.1101/443747.
Razy-Krajka, F., Lam, K., Wang, W., Stolfi, A., Joly, M., Bonneau, R., Christiaen, L., 2014. Collier/OLF/EBF-dependent transcriptional dynamics control pharyngeal muscle specification from primed cardiopharyngeal progenitors. Dev. Cell. 29, 263–276.
Reeves, W.M., Wu, Y., Harder, M.J., Veeman, M.T., 2017. Functional and evolutionary insights from the *Ciona* notochord transcriptome. Development 144, 3375–3387.
Roure, A., Darras, S., 2016. Msxb is a core component of the genetic circuitry specifying the dorsal and ventral neurogenic midlines in the ascidian embryo. Dev. Biol. 409, 277–287.
Sakurai, S., Shimizu, T., Ohto, U., 2017. The crystal structure of the AhRR-ARNT heterodimer reveals the structural basis of the repression of AhR-mediated transcription. J. Biol. Chem. 292, 17609–17616.
Satoh, N., Tagawa, K., Takahashi, H., 2012. How was the notochord born? Evol. Dev. 14, 56–75.
Satou, Y., Mineta, K., Ogasawara, M., Sasakura, Y., Shoguchi, E., Ueno, K., Yamada, L., Matsumoto, J., Wasserscheid, J., Dewar, K., et al., 2008. Improved genome assembly and evidence-based global gene model set for the chordate *Ciona intestinalis*: new insight into intron and operon populations. Genome Biol. 9, R152.
Satou, Y., Takatori, N., Yamada, L., Mochizuki, Y., Hamaguchi, M., Ishikawa, H., Chiba, S., Imai, K., Kano, S., Murakami, S.D., Nakayama, A., Nishino, A., Sasakura, Y., Satoh, G., Shimotori, T., Shin-I, T., Shoguchi, E., Suzuki, M.M., Takada, N., Utsumi, N., Yoshida, N., Saiga, H., Kohara, Y., Satoh, N., 2001. Gene expression profiles in *Ciona intestinalis* tailbud embryos. Development 128, 2893–2904.
Shinohara, M., Terada, Y., Iwamatsu, A., Shinohara, A., Mochizuki, N., Higuchi, M., Gotoh, Y., Ihara, S., Nagata, S., Itoh, H., Fukui, Y., Jessberger, R., 2002. SWAP-70 is a guanine-nucleotide-exchange factor that mediates signalling of membrane ruffling. Nature 416, 759–763.
Suzuki, M., Sato, F., Bhawal, U.K., 2014. The basic helix-loop-helix (bHLH) transcription factor DEC2 negatively regulates Twist1 through an E-box element. Biochem. Biophys. Res. Commun. 455, 390–395.
Takahashi, H., Hotta, K., Erives, A., Di Gregorio, A., Zeller, R.W., Levine, M., Satoh, N., 1999. Brachyury downstream notochord differentiation in the ascidian embryo. Genes Dev. 13, 1519–1523.
Tolkin, T., Christiaen, L., 2016. Rewiring of an ancestral Tbx1/10-Ebf-Mrf network for pharyngeal muscle specification in distinct embryonic lineages. Development 143, 3852–3862.
Wang, L.H., Baker, N.E., 2015. E proteins and ID proteins: helix-loop-helix partners in development and disease. Dev. Cell. 35, 269–280.
Xia, B., Fang, S., Chen, X., Hu, H., Chen, P., Wang, H., Gao, Z., 2016. MLKL forms cation channels. Cell Res. 26, 517–528.
Yamada, L., Kobayashi, K., Satou, Y., Satoh, N., 2005. Microarray analysis of localization of maternal transcripts in eggs and early embryos of the ascidian *Ciona intestinalis*. Dev. Biol. 284, 536–550.
Zeller, R.W., Weldon, D.S., Pellatiro, M.A., Cone, A.C., 2006. Optimized green fluorescent protein variants provide improved single cell resolution of transgene expression in ascidian embryos. Dev. Dyn. 235, 456–467.